MICROSCOPIC DISPLACEMENT OF BITUMEN DURING SOLVENT-STEAM-FLOODING: EFFECTS OF RESERVOIR CLAYS AND SOLVENT TYPE

A Thesis

by

RAPHAEL SALLES DA COSTA COELHO

Submitted to the Office of Graduate and Professional Studies of
Texas A&M University
in partial fulfillment of the requirements for the degree of

MASTER OF SCIENCE

Chair of Committee,	Berna Hascakir
Co-Chair of Committee,	Maria Barrufet
Committee Member,	Hadi Nasrabadi
Head of Department,	A. Daniel Hill

May 2016

Major Subject: Petroleum Engineering

ABSTRACT

Solvent-steam-flooding (SSF) processes have several advantages over steam-flooding for bitumen extraction. It is well known that the addition of solvent increases oil production and mitigates environmental impacts due to steam generation. However, there exist numerous unknowns on the mutual interactions of solvent with steam, reservoir oil, and reservoir rock which affect the overall performance of the EOR method.

Through an experimental approach, this study investigates the microscopic displacement efficiency of SSF for the extraction of Peace River bitumen.

Two types of gas phase solvents were tested: hydrocarbon (propane) and non-hydrocarbon (carbon dioxide - CO_2). Propane was chosen for its good solubility in oil, whereas CO_2 was selected as an environmentally friendly option to decrease the project's carbon footprint by re-injecting boiler combustion or associated gas.

Solvent flooding (CO_2 flooding and propane flooding), steam-flooding, and SSF performances to extract Peace River bitumen were investigated with 12 one-dimensional core flooding experiments. Process performances were evaluated with cumulative oil recovery, sweep efficiency, produced oil and residual oil quality analyses.

To investigate the effect of reservoir fines (clays), experiments were performed with and without clays on the reservoir rock. The phase behavior of the solvent-crude-asphaltene interactions was also studied by analyzing asphaltene precipitation. Finally, the impacts of varying the solvent flowrate were also studied.

This research study suggests that CO_2 or propane insoluble fractions (asphaltenes) decrease permeability and increase oil viscosity during solvent flooding due to their interactions with clays. These problems are enhanced by solvent-steam co-injection, which also causes the formation of emulsions. Clay migration to oil phase during production is more significant for propane-steam co-injection. It is believed that the polar nature of asphaltenes is the reason behind the interactions with clays and water.

DEDICATION

This thesis is dedicated to my parents, Valéria and Paulo, and to my brother, João Marcos, for their endless support and deep devotion to my personal growth. I am eternally grateful for being guided by them.

ACKNOWLEDGEMENTS

I would like to thank my advisor, Dr. Berna Hascakir, for her continuous support throughout my research. I would also like to thank my co-advisor, Dr. Maria Barrufet, and Dr. Nasrabadi for their willingness to serve as my committee members.

The financial support and the opportunity provided by my sponsor, CAPES, Coordenação de Aperfeiçoamento de Pessoal de Nível Superior – Brasil, and by this research project sponsor, Chevron Corporation, are also greatly appreciated.

I am also thankful for the members of the Heavy Oil, Oil shales, Oil sands, & Carbonate Analysis and Recovery Methods Research Team at the Texas A&M University Petroleum Engineering Department for their help during my research.

NOMENCLATURE

C_3	Propane
CCS	Carbon Capture and Sequestration
CPA-EOS	Cubic-Plus-Association Equation-of-State
CWE	Cold water equivalent
DAO	De-Asphalted Oil
EOR	Enhanced Oil Recovery
ES-SAGD	Expanding-Solvent-Steam-Assisted Gravity Drainage
GHG	Greenhouse Gas
HSE	Health, Safety and Environment
LPG	Liquefied Petroleum Gas
PR-EOS	Peng Robinson Equation-of-State
R^2	Coefficient of Determination
SAGD	Steam-Assisted Gravity Drainage
SF	Steam-Flooding
SSF	Solvent-Steam-Flooding
TGA/DSC	Thermogravimetric Analysis/Differential Scanning Calorimetry

TABLE OF CONTENTS

Page

ABSTRACT ii

DEDICATION iv

ACKNOWLEDGEMENTS v

NOMENCLATURE vi

TABLE OF CONTENTS vii

LIST OF FIGURES ix

LIST OF TABLES xi

CHAPTER I INTRODUCTION AND LITERATURE REVIEW 1

CHAPTER II MATERIALS AND METHODS 9

1. Sample Preparation 9
2. Core Flooding Experimental Procedure 10
3. Produced Oil and Spent-Rock Analyses 12

CHAPTER III RESULTS AND DISCUSSIONS 16

1. Recovery Performance 16
2. Rheology 21
3. Asphaltene, Clay, and Water Content 26
4. Spent-Rock Analysis 30

CHAPTER IV CONCLUSIONS 36

REFERENCES 38

APPENDIX A CONTROL TGA/DSC RESULTS FOR DISTILLED WATER 47

APPENDIX B RHEOLOGICAL BEHAVIOR OF PRODUCED OIL 48

APPENDIX C TGA/DSC RESULTS 51

APPENDIX D PHASE BEHAVIOR CALCULATIONS 60

APPENDIX E REPEATABILITY.....65

LIST OF FIGURES

Page

Figure 1. Schematic diagram of the experimental setup. 11

Figure 2. Cumulative oil recovery (clays and water excluded). 17

Figure 3. Oil production rates (clays and water excluded). 18

Figure 4. Microscopic pictures of water-in-oil emulsions. 400× magnification. 19

Figure 5. Produced oil viscosities as a function of temperature. 23

Figure 6. Relationship between Power-Law regression constants from Table 4. Dashed lines indicate trend lines. 24

Figure 7. Effect of clays on Peace River bitumen viscosity. 26

Figure 8. Produced oil composition, considering clays, asphaltenes, DAO, and water. 28

Figure 9. Normalized produced oil sample composition, considering only the presence of DAO and asphaltenes (water and clays excluded). 29

Figure 10. Spent-rock pictures. 31

Figure 11. Residual oil composition, including clays. 34

Figure A-1. TGA/DSC analysis of distilled water. 47

Figure B-1. Comparison of calculated and measured viscosities of produced oil samples (experiments E1, E2, E3, E4, E5, and E6). 49

Figure B-2. Comparison of calculated and measured viscosities of produced oil samples (experiments E7, E8, E9, E10, E11, and E12). 50

Figure C-1. TGA/DSC analysis of produced oil samples from solvent flooding experiments (E2, E3, E9, and E10). 52

Figure C-2. TGA/DSC analysis of produced oil samples from steam and solvent-steam-flooding experiments (E1, E6, E7, E8, E11, and E12). 53

Figure C-3. TGA/DSC analysis of produced oil samples from steam and propane-steam-flooding experiments (E1, E4, E5, and E6). 54

Figure C-4. TGA/DSC analysis of precipitated asphaltenes from solvent flooding experiments without clays. 55

Figure C-5. TGA/DSC analysis of postmortem samples from experiments E1, E2, and E3. 56

Figure C-6. TGA/DSC analysis of postmortem samples from experiments E4, E5, and E6. 57

Figure C-7. TGA/DSC analysis of postmortem samples from experiments E7, E8, and E9. 58

Figure C-8. TGA/DSC analysis of postmortem samples from experiments E10, E11, and E12. 59

Figure D-1. Simulated pseudo-ternary diagrams to visualize different solubility behaviors of propane and CO_2 with Peace River bitumen. 64

Figure E-1. Cumulative oil recovery (clays and water excluded) for repeated experiments. 65

LIST OF TABLES

Page

Table 1. Peace River fluid properties 9

Table 2. Experimental conditions summary for the 12 core flooding experiments. 13

Table 3. Solvent to steam volumetric, molar, and mass ratios during SSF. 13

Table 4. Power-Law equations regressed for produced oil viscosities. 24

Table 5. Residual oil saturations. 32

Table 6. Calculated microscopic sweep efficiency. 33

Table B-1. Regressed flow consistency and flow behavior indexes for produced oil samples. 48

Table D-1. Peace River pseudo-component fluid properties 60

Table D-2. Estimated solubilities for propane and CO_2 in Peace River dead oil. 62

CHAPTER I

INTRODUCTION AND LITERATURE REVIEW

Oil is predicted to remain the most demanded energy source in the next three decades, experiencing a demand increase of almost 30% as a result of increasing industrial activity, population growth, and energy consumption (ExxonMobil, 2013). Simultaneously, the emissions of carbon dioxide (CO_2) and other greenhouse gases (GHG) are projected to dramatically surge (Marchal et al., 2011). Therefore, the petroleum industry must develop environmentally and technically feasible oil recovery methods to meet such demands.

Bitumen reserves account for 30% of the world's oil reserves (Alboudwarej et al., 2006). Over 1.7 trillion barrels of these reserves are located in Alberta, Canada) Hein and Marsh, 2008). In the Peace River area, located northwestern Alberta, the bitumen reserves are estimated at approximately 0.13 trillion barrels (Hein and Marsh, 2008).

Nonetheless, the extraction of these resources is challenging due to the extremely high viscosity of bitumen (above 10,000 cP at reservoir temperature), which usually requires thermal Enhanced Oil Recovery (EOR) methods to increase oil mobility in the reservoir (Prats, 1982; Green and Willhite, 1998).

Steam-flooding is a reliable process of introducing heat and drive energy to the reservoir, being under field commercial application since the 1960s (Green and Willhite, 1998). The main recovery mechanisms developed during steam stimulation are viscosity

reduction, emulsions drive, thermal expansion, solution gas drive, and steam distillation (Prats, 1982; Green and Willhite, 1998; Speight, 2009).

However, steam injection for bitumen extraction has high environmental impacts due to excessive amounts of fresh water consumption and GHG emissions. Moreover, heat losses, poor injectivity, reservoir depth, and high mobility ratios make this process unfavorable (Speight, 2009; Huc, 2011).

To overcome the drawbacks of steam-flooding, hybrid miscible-thermal methods to extract bitumen were first proposed by Hernandez and Farouq Ali (1972), who observed increased oil recovery factors after co-injecting steam with liquid solvents, such as toluene and naphtha.

As several solvents may be added to steam-flooding, the choice for the most appropriate solvent for each potential field application must follow economic and technical criteria.

Considering the long term sustainability of a field project, the main economic criteria that guide solvent choice are stable supply and cost throughout the project life (Frauenfeld et al., 2009; Keshavarz et al., 2015).

Since CO_2 emissions are unwanted due to their impacts on climate change, CO_2 is considered an environmentally friendly alternative as an EOR fluid. Though CO_2 emissions are high, CO_2 capturing is difficult and expensive. Hence, it is useful to report possible CO_2 sources for SSF projects.

CO_2 production by anthropogenic activities are expected to increase from 30 Gtons in 2010 to 55 Gtons/year in 2050 (Marchal et al., 2011). In the same period, CO_2 emissions

in the U.S. are projected to be stable at approximately 5.5 Gtons/year (EIA, 2015). However, the Canadian CO_2 emissions are estimated to grow from 0.70 to 0.73 Gton from 2010 to 2020, with Alberta being responsible for approximately 37% of the total emissions (ECCC, 2013; Bachu, 2016). In Canada, the heavy oil and bitumen thermal extraction plants have a huge carbon footprint, producing approximately 85 kg CO_2/bbl for steam-based methods (ECCC, 2013).

Propane is another solvent widely available for SSF. For the supply to an oilfield operation, propane can be obtained from three sources: associated gas, non-associated gas, and by refined liquefied petroleum gas (LPG) (IHS, 2012). Therefore, the propane price and supply sustainability to any EOR field application are directly related to oil and natural gas production trends, as well as to refining activities (IHS, 2012).

In the next decades, propane supply is expected to be stable in North America due to the recent rise of the shale gas plays, which are estimated to produce approximately 0.8 MBPD of propane by 2020 (IHS, 2012). In Canada, propane supply is also expected to remain relatively constant in the next decades as the country historically produces large surplus amounts of the product, which are then exported to the U.S.

In perspective, the propane supply in Canada is projected to achieve 0.17 MBPD in 2020, with approximately 55% of this production being destined to external markets (Goobie and Kelly, 2012). Considering that the Canadian exports to the U.S. may decrease due to the supply from American shale gas, more propane would be available for the Canadian bitumen and heavy oil plays for SSF projects.

Additionally, it is also expected that the propane supply will be affected in the short-term due to low crude oil prices, which achieved approximately US$30 by the beginning of 2016 (NASDAQ, 2016).

However, CO_2 is more widely available than propane, as CO_2 is originated from industrial, agricultural, and transportation activities, naturally from CO_2 reservoirs, as well as from associated and non-associated natural gas (Metz et al., 2005). However, the CO_2 storage and selling market is still limited worldwide (Metz et al., 2005; Bachu, 2016).

The existence of a solvent supply infrastructure must also be taken into account. Considering this aspect, propane has a competitive advantage over CO_2. Due to the much lower vapor pressure of propane (McCain, 1990), it can easily be transported either by pipelines or in the higher density liquefied state by road, rail, or marine tankers, whereas CO_2 is generally transported by pipelines (Metz et al., 2005).

One great advantage of using CO_2 is related to the possibility of coupling EOR and Carbon Capture and Sequestration (CCS) projects, simultaneously increasing oil production and reducing GHG emissions (Bachu, 2016). Despite the higher availability of CO_2 than propane, its utilization also presents economic limitations, mainly because CO_2 capturing and purification is expensive. Currently, the available technologies usually cost 12-60 US$/tonne-$CO_2$ and account for two-thirds of the CCS project cost (Metz et al., 2005; Bybee, 2008).

Particularly in the Alberta region, 29 oilfields were found suitable for CO_2-EOR and CCS, with a potential of approximately 1.6 billion incremental barrels and 780 Mton of CO_2 storage (Bachu, 2016). However, it is worth mentioning that shallow (less than

1000 m) and depleted reservoirs subject to thermal recovery methods are not commonly considered for CO_2 storage, as the reservoir pressure and temperature hinder the achievement of supercritical CO_2 (Bachu and Stewart, 2002; Shaw and Bachu, 2003). CO_2 injection on supercritical state is preferred for storage to achieve higher densities and to avoid separation into gas and liquid phases (Pruess et al., 2003; Metz et al., 2005).

Therefore, CO_2 storage in bitumen reservoirs would not be effective during SSF in Peace River, where typical reservoir depths are 550 m (Hamm and Ong, 1995). However, the option for CO_2 could still be environmentally friendly considering the possibility of capturing CO_2 directly from steam generators and surface upgrading facilities, followed by purification and injection to the reservoir (Ordorica-Garcia et al., 2012).

Another option to offset the capturing and purification costs would be the re-injection of fractions of associated gas. In this case, the usage of CO_2 in the Peace River area is more competitive than propane as the associated gas from these reservoirs are CO_2-rich and poor in gaseous alkanes, having an average composition of 65.8 mole% of CO_2 and 1.2 mole% of propane (Hitchon, 1963; Svrcek and Mehrotra, 1989).

For either propane or CO_2, another economic factor that must be considered is solvent trapping, as fractions of the injected fluid are expected to remain immobile either in the residual reservoir fluids or in the pore-throats, becoming unavailable for re-injection (Metz et al., 2005; Juanes et al., 2006; Pentland et al., 2011; Naderi and Babadagli, 2014; Coelho and Hascakir, 2015).

Considering the technical aspects, the solvent choice must consider toxicity, solvent phase in reservoir conditions, and recovery mechanisms.

Low solvent toxicity is preferred to mitigate health, safety, and environmental (HSE) risks. Propane is non-toxic to animals, plants, soils, and water, with HSE risks mostly related to flammability and suffocation (Carson and Mumford, 2002). Carbon dioxide, however, affects water pH, is a GHG, and is toxic to human beings and plants (NIOSH, 1976; Carson and Mumford, 2002; Metz et al., 2005). Nevertheless, both CO_2 and propane are less toxic than solvents tested in previous works, such as toluene, hexane, and naphtha (Scheflan and Jacobs, 1953; Mukhametshina et al., 2015).

The solvent phase in reservoir and surface conditions is also key for solvent selection for SSF projects. Gaseous solvents are advantageous in the reservoir as they expand with steam, providing mechanical gas drive to the oil (Stone and Malcolm, 1985; Hornbrook et al., 1991; Gumrah and Bagci, 1997). In the surface facilities, gas-phase solvents are also preferred as separation from produced oil for solvent re-injection is easier than for liquid solvents (Shu and Hartman, 1988; Li and Mamora, 2010).

Finally, the bitumen macroscopic (volumetric) and microscopic (pore-scale) displacement mechanisms provided by each solvent must also be addressed.

Numerous experimental and simulation studies have focused on the macroscopic efficiency of SSF for bitumen extraction. These works found that solvent-steam co-injection introduces recovery mechanisms such as miscible displacement, oil-foaming, gas drive, viscosity reduction, and oil stripping (Farouq Ali and Abad, 1976; Redford and McKay, 1980; Stone and Ivory, 1987; Nasr et al., 1987; Mohammed and Babadagli, 2015).

These studies also demonstrate that such synergetic macroscopic recovery mechanisms of steam and solvent expedite production and increase recovery factors. These observations justify the technical and environmental reasoning of SSF, as the faster bitumen production decrease steam generation requirements and GHG emissions.

Nonetheless, knowledge of microscopic displacement mechanisms controlling bitumen extraction efficiency through SSF is also of paramount relevance. Complex pore-scale interactions between bitumen, reservoir fines (clays), water, and solvents must be investigated as they exert major controls on the microscopic sweep efficiency and on the produced oil quality (Ezeuko et al., 2013; Kar et al., 2015; Mukhametshina et al., 2015).

The usage of solvents may cause different types and intensities of asphaltene precipitation (Mitchell and Speight, 1973; Monger and Trujillo, 1991). The works by Mohammadzadeh et al. (2010), Moreno-Arciniegas and Babadagli (2014), and Mukhametshina et al. (2015) identified that different types of solvents control the dynamics of asphaltene precipitation, which ultimately affects the recovery performance, produced oil quality, and rock wettability.

Ezeuko et al. (2013) studied the formation of emulsions during steam-assisted gravity drainage (SAGD) and recognized them as crucial to bitumen displacement. Naderi and Babadagli (2014), who studied alternating steam with propane and CO_2, found that the recovery efficiency of each solvent is controlled by wettability and pore size.

Solvent-bitumen interactions will also be affected by the presence of reservoir fines (clays), which are known to interact with asphaltenes and water (Leontaritis et al., 1994). These interactions affect oil displacement and solvent trapping in the reservoir

(Coelho and Hascakir, 2015; Kar and Hascakir, 2015; Wang and Leung, 2015), and were recognized to be controlled by clay type (Kar et al., 2015).

The present work expands these analyses and investigates the effects of solvent type and flowrate on bitumen extraction through SSF. Gas phase asphaltene insoluble hydrocarbon (propane) and non-hydrocarbon (CO_2) solvents are tested. The role of reservoir clays on the microscopic displacement efficiency is also studied.

CHAPTER II

MATERIALS AND METHODS

1. Sample Preparation

12 core flooding experiments were performed on a bitumen sample from the Peace River region, located Northwestern Alberta, Canada. The bitumen properties are presented in Table 1.

To investigate the effect of clays on bitumen extraction, the reservoir rock was prepared either with only Ottawa sand or with an Ottawa sand-clay mixture.

For the sand-clay mixture, 15 wt% clays (2.3 μm average particle size) is mixed with 85 wt% Ottawa sand (425 to 850 μm particle size) (Kar et al., 2015). This mixture represents the clay-rich Peace River reservoirs (Bayliss and Levinson, 1976; Wightman et al., 1989). The clays used in this study are a mixture of 90 wt% kaolinite and 10 wt% illite (Kar et al., 2015).

While the sand-only reservoir rock corresponds to 39.1% porosity and represents clean-sand portions like the Bluesky formation (Wightman et al., 1989; Smith et al., 2009; Vannaxay et al., 2014), the sand-clay mixture corresponds to 32% porosity.

Table 1. Peace River fluid properties (Mukhametshina et al., 2015).

Property, unit	Value
Oil gravity, °API[*]	8.8
Oil viscosity (at 20°C), cP	54,152
Oil asphaltene content, wt%[†]	34.3

[*]API gravity is given at standard conditions (API, 1980).
[†]Asphaltenes are *n*-pentane insoluble.

For both reservoir rock types, the pore space was filled with 84 vol% bitumen and 16 vol% distilled water to reproduce typical reservoir saturations (Hamm and Ong, 1995).

2. Core Flooding Experimental Procedure

The pore-scale displacement was investigated with 12 experiments by using 1-D core flooding apparatus which mimics piston-like displacement. The oilsand mixtures were packed in a stainless steel cylinder core holder (19 cm height, 5.4 cm inner diameter, and 9.8 cm outer diameter), designed to study core flooding experiments in pore-scale (Figure 1). The packing procedure followed the methodology by Mukhametshina et al. (2015).

The cell outlet was equipped with a 210 μm size metal screen to avoid sand production. The core holder was completely sealed with stainless steel caps, insulated with fiberglass cloths, and the internal temperature was measured by a single thermowell with two thermocouples. The thermocouples were placed 5 and 10 cm below of injection point. The experiments with steam were conducted at 115°C and 15 psig injection pressure, whereas those with pure solvent injection were ran at 20°C to mimic the approximate reservoir temperature of 17°C (Hamm and Ong, 1995).

Piston-like displacement was achieved by conducting experiments vertically. Experiments were conducted by injecting steam and/or high purity gas phase solvents. Water was pumped by an ISCO syringe pump to a steam generator, which converts water to steam and directly injects the stream to the core holder cell. Propane and CO_2 were injected directly from solvent cylinders with 100 psig injection pressure. The cell back pressure was kept constant at atmospheric pressure to maintain flow.

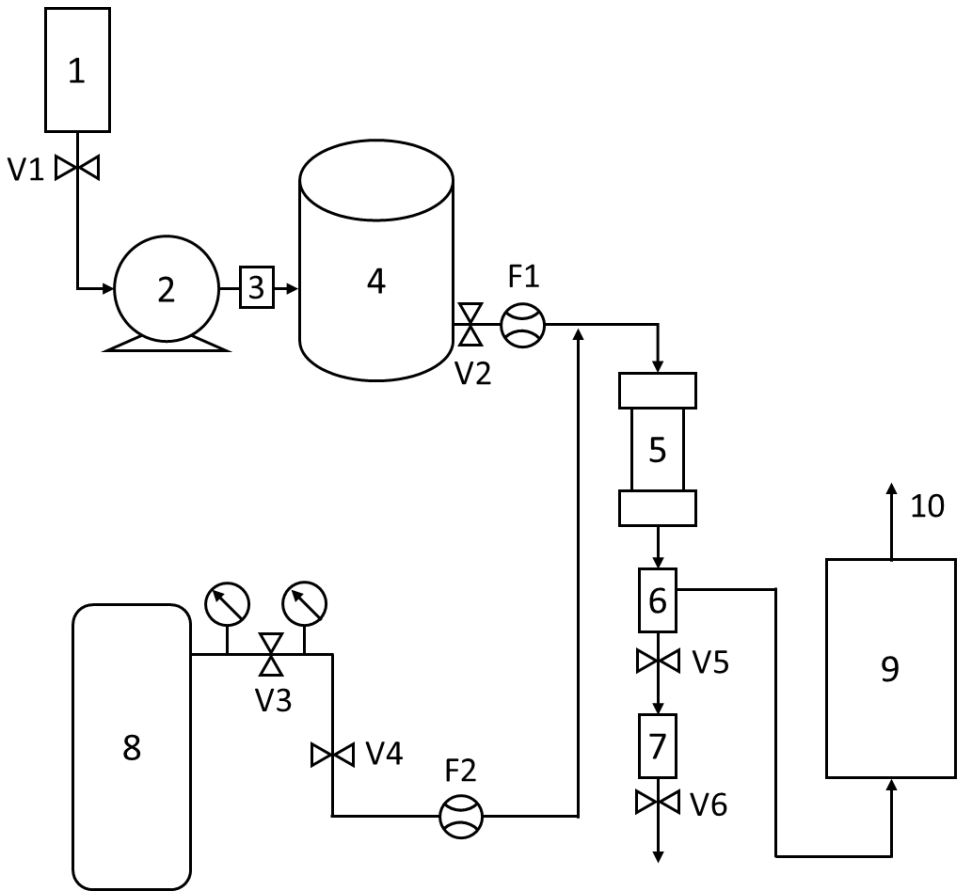

1 -	Distilled water cylinder	10 -	Gas outlet to vent
2 -	ISCO syringe water pump	V1 -	Water injection valve
3 -	Water backpressure regulator	V2 -	Steam injection valve
4 -	Steam generator	V3 -	Solvent injection valve 1
5 -	Core holder	V4 -	Solvent injection valve 2
6 -	Separator	V5 -	Produced fluids valve 1
7 -	Sampler	V6 -	Produced fluids valve 2
8 -	Solvent cylinder	F1 -	Steam line one-way valve
9 -	Condenser	F2 -	Solvent line one-way valve

Figure 1. Schematic diagram of the experimental setup.

The gas solvent flowrate was controlled by a gas rotameter model Cole Parmer EW-03217-12. Two one-way check valves were installed on the steam generator and solvent injection lines to avoid backflow.

Produced oil, water, solvent, and steam were directed first to a separator and then to a condenser, which was placed into a water bath. The remaining vapors were vented.

The experimental conditions for the 12 experiments are summarized in Table 2. Table 3 presents the solvent to steam volumetric, molar, and mass ratios during SSF.

The first experiments (E1, E2, and E3) were conducted to investigate the impact of steam, propane, and CO_2 flooding on bitumen extraction with the presence of clays. Then, to investigate the impacts of clays on recovery performance, these experiments were repeated without clay addition (E8, E9, and E10).

Solvent-steam experiments were conducted to investigate the impact of solvent concentration and clay presence in SSF performance. For propane-steam, three different solvent flowrates were tested (E4, E5, and E6). The highest flowrate case was also tested for CO_2-steam (E7). The impact of clay during SSF was investigated by repeating propane-steam and CO_2-steam flooding without clays (E11 and E12).

3. Produced Oil and Spent-Rock Analyses

Propane and CO_2 are asphaltene insoluble solvents (Mitchell and Speight, 1973; Mungan, 1981). Thus, after each core flooding experiment, produced oil and postmortem (spent-rock) samples were analyzed to better understand the role of asphaltenes in pore-scale displacement.

Table 2. Experimental conditions summary for the 12 core flooding experiments.

Experiment	Sand : Clay, wt%	EOR Method	Injected Fluids	Solvent to Steam* Injection Rate, cc/min	Experimental Temperature, °C
E1	85:15	SF	Steam	0:18	115
E2	85:15	Solvent flooding	C_3	18:0	20
E3	85:15	Solvent flooding	CO_2	18:0	20
E4	85:15	SSF	C_3-Steam	1:9	115
E5	85:15	SSF	C_3-Steam	1:1	115
E6	85:15	SSF	C_3-Steam	9:1	115
E7	85:15	SSF	CO_2-Steam	9:1	115
E8	100:0	SF	Steam	0:18	115
E9	100:0	Solvent flooding	C_3	18:0	20
E10	100:0	Solvent flooding	CO_2	18:0	20
E11	100:0	SSF	C_3-Steam	9:1	115
E12	100:0	SSF	CO_2-Steam	9:1	115

*Solvent and steam rates are reported at 20˚C and 14.7 psi.

Table 3. Solvent to steam volumetric, molar, and mass ratios during SSF.

Experiment	Injected Fluids	Solvent to Steam* Ratio, vol/vol	Solvent to Steam Ratio, mole/mole	Solvent to Steam Ratio, mass/mass
E4	C_3-Steam	1:9	1:1199	1:626
E5	C_3-Steam	1:1	1:171	1:70
E6	C_3-Steam	9:1	1:19	1:7.8
E7	CO_2-Steam	9:1	1:21	1:8.6
E11	C_3-Steam	9:1	1:19	1:7.8
E12	CO_2-Steam	9:1	1:21	1:8.6

*Solvent and steam volumes are reported at 20˚C and 14.7 psi.

The produced oil quality was assessed with rheological, Thermogravimetric Analyzer/Differential Scanning Calorimetry (TGA/DSC), asphaltene content, and clay content measurements.

Rheological studies were performed using a Brookfield HBDV-III rheometer through shear stress and stress rate measurements with varying torques. Viscosity measurements were conducted from 30 to 80°C.

The water content of produced oil samples was estimated by heating oil samples using TGA/DSC with air injection. Water evaporation can be identified in the DSC curve with an endothermic peak at approximately 150°C, as observed for distilled water (Figure A-1, Appendix A). Therefore, the water content corresponds to the weight loss observed on the TGA curve until 150°C.

Asphaltene content of produced oil samples was measured by using *n*-pentane dissolution according to ASTM D2007-11 procedure (ASTM, 2011), followed by toluene wash to determine clay content (Amyx et al., 1960; Kar and Hascakir, 2015).

Spent-rock analyses were also performed. For the rocks used in this study, the clay mixture average particle size is 2.3 µm, while the Ottawa sand particle size ranges from 425 to 850 µm (Kar et al., 2015).

First, residual oil was extracted by washing the spent-rock with *n*-pentane, which allows asphaltene and spent-rock separation from de-asphalted oil (DAO), using a 20-25 µm filter paper. Secondly, the spent rock was washed with toluene using the same 20-25 µm filter paper to remove asphaltenes and clays attached to asphaltenes (Amyx et al.,

1960; Kar and Hascakir, 2015). Lastly, the diluted DAO-clay and asphaltene-clay solutions were filtered on a <2 μm filter paper to remove clays.

TGA/DSC was also used to determine water and residual oil saturations. The spent rock samples were combusted by using 5°C/min heating rate until reaching 800°C. The residual water content is computed as the mass loss until 150°C, whereas the residual oil content is considered as the mass loss observed from 150 to 800°C.

It should be noted the residual water saturation may not be exact since TGA/DSC measurements were not carried out right after each experiment. Therefore, there might exist some errors due to water evaporation before TGA/DSC measurements.

CHAPTER III

RESULTS AND DISCUSSIONS

1. Recovery Performance

To assess the performance of each EOR method, cumulative oil recoveries and oil production rates were recorded during the experiments. These results are summarized in Figures 2 and 3. The produced oil reported in Figures 2 and 3 is free from water-in-oil emulsions and clays. The performance results are discussed considering the effect of clay presence in the reservoir, type of solvent, and solvent flowrate.

1.1. Effect of Clay Presence in Reservoir Rock

Figures 2a, 2b, 3a, and 3b present results for the experiments conducted with reservoir rocks prepared with clay addition (E1, E2, E3, E6, and E7), reported in solid curves, and for those conducted with the reservoir rocks containing only sand (E8 through E12), reported in dashed lines.

Results indicate that the presence of clays (with 2.3 μm average particle size) in the reservoir has a strong negative effect to the Peace River bitumen recovery performance by drastically reducing the final recovery factors and delaying production profiles. These observations are valid for solvent, steam, and solvent-steam flooding experiments.

These effects are justified by clay dispersion in sandstones, as well as by clay-water, clay-asphaltene, and solvent-crude interactions (Neasham, 1977; Redford and McKay, 1980; Leontaritis et al., 1994; Kar et al., 2015; Coelho and Hascakir, 2015).

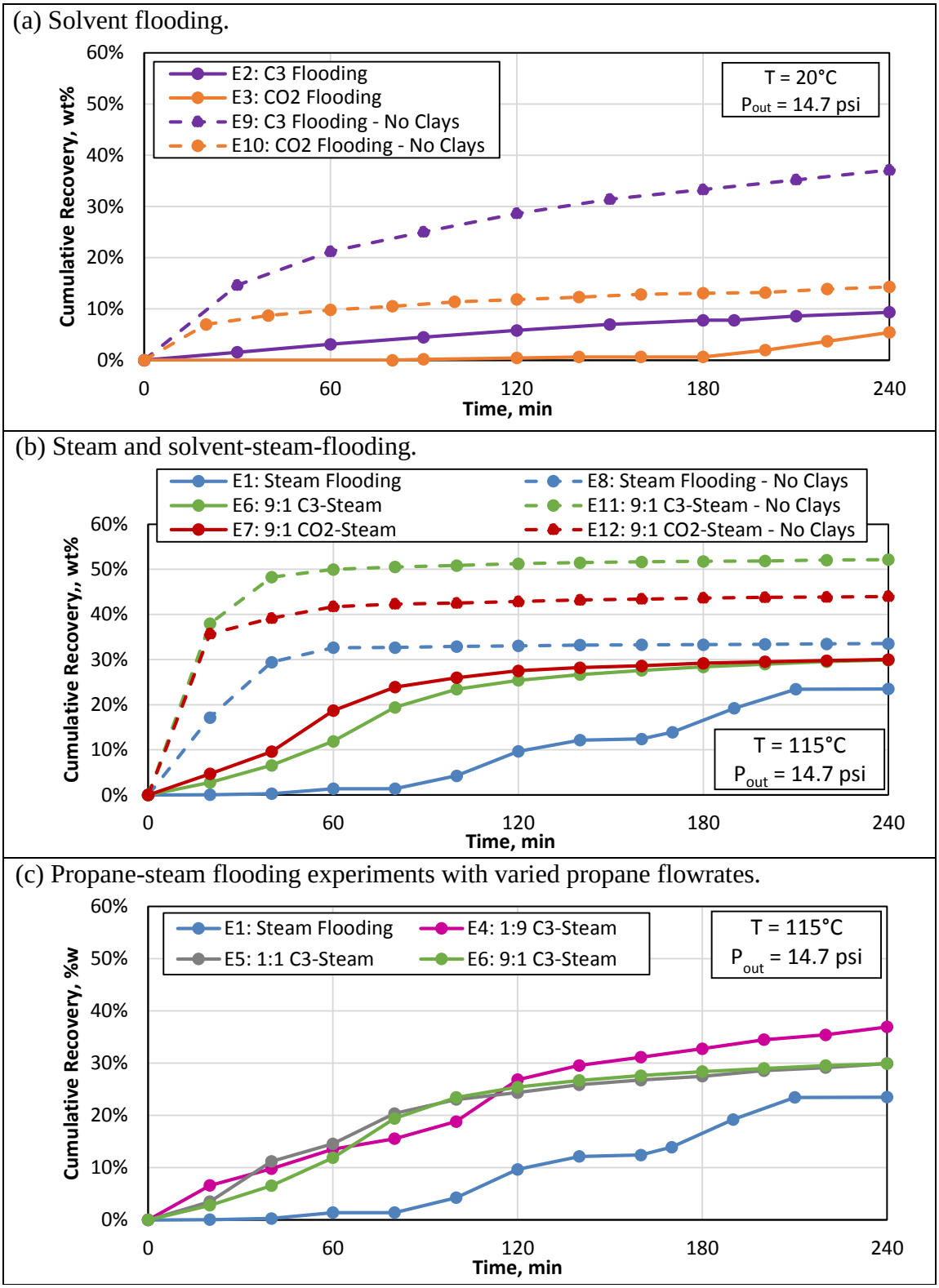

Figure 2. Cumulative oil recovery (clays and water excluded).

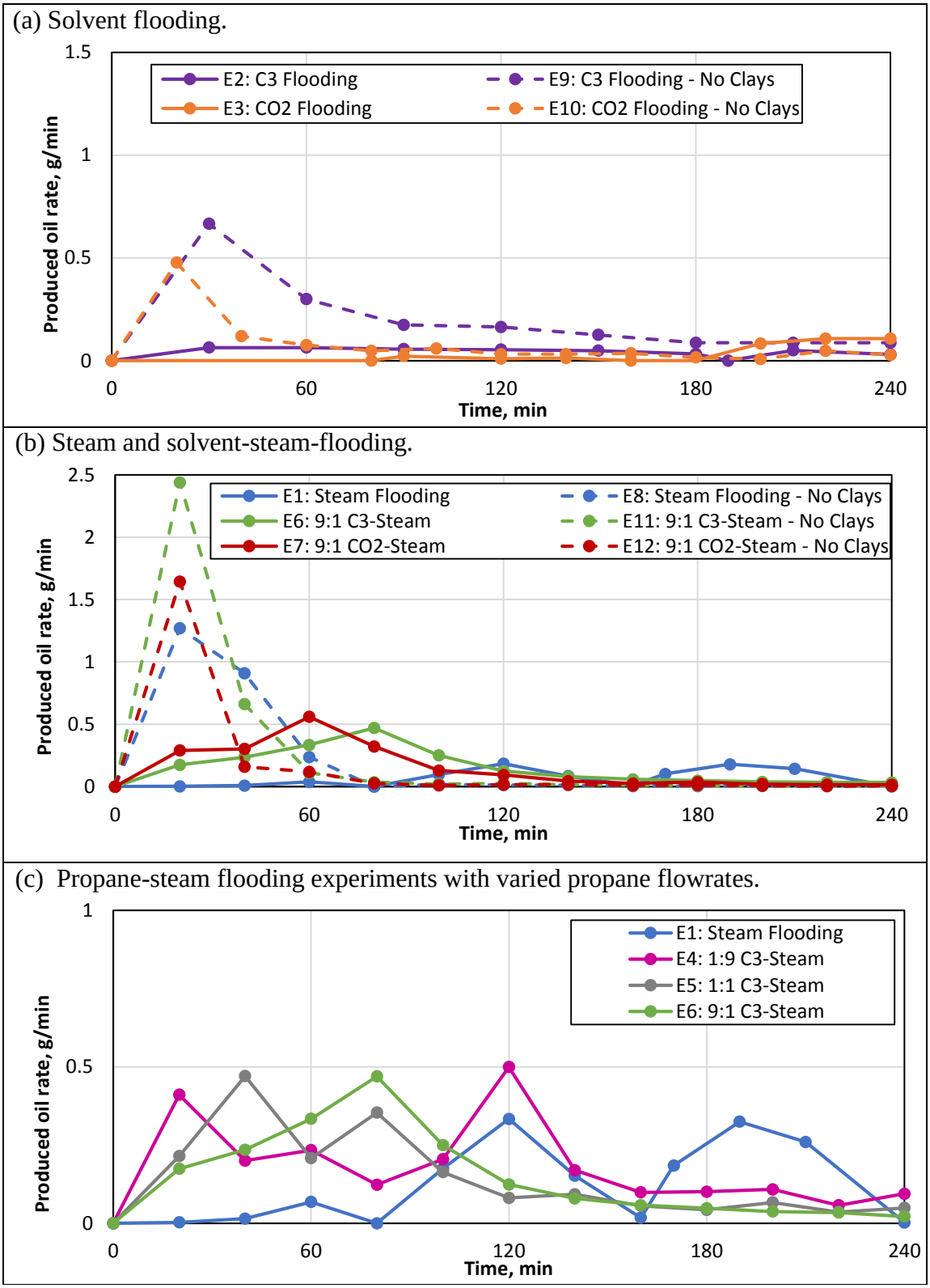

Figure 3. Oil production rates (clays and water excluded).

It must be noted that the clays used in E1 through E7 are a mixture of kaolinite and illite. Kaolinite causes pore-filling by occupying the sandstone inter-granular pores, reducing pore volume and acting as migrating fines in the reservoir (Neasham, 1977).

Illite may attach to the sand grains surfaces (pore-lining) and extend across pores and pore-throats (pore-bridging), creating micro-porosity and tortuous flow paths. The combination of such features reduce relative permeabilities and porosity, and increase capillary pressures (Neasham, 1977, Kar et al., 2015).

Illite-water interaction also occurs due to the high polarity of both species, which cause them to associate, swell, and cement with the sand grains, also reducing permeability (Bil et al., 1988; Hughes et al., 1989; Kar et al., 2015).

Such illite-water interactions may also justify why solvent injection experiments without clays (E9 and E10) had water displaced as a separate phase from oil by gas drive and solubility (Wiebe and Gaddy, 1940; Kobayashi and Katz, 1953). When clays were present (E2 and E3), only single phase water-in-oil emulsions were produced (Figure 4), as the connate water became immobile due to cementation with illite.

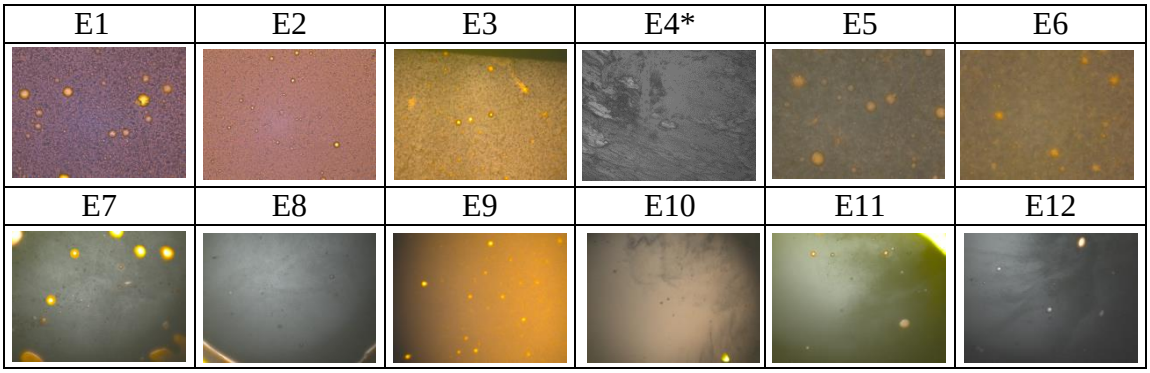

Figure 4. Microscopic pictures of water-in-oil emulsions. 400× magnification.
*Sample E4 solidified before microscopic imaging, therefore no emulsions can be seen.

Additionally, clay-asphaltene interactions enhance asphaltene flocculation and precipitation, which may promote pore-throat clogging, permeability reduction, and wettability alteration (Leontaritis et al., 1994). Such effects may be augmented due to injection of asphaltene insoluble solvents such as propane and CO_2 (Mungan, 1981; Speight, 2006; Deo and Parra, 2012; Coelho and Hascakir, 2015).

The negative effects of clays to crude oil recovery performance were also recognized by Smith et al. (2009) on the clay-rich (80-90%) portions of the Peace River reservoirs. However, the present work demonstrates that even at lower clay contents (15 wt%), the recovery performance might be drastically reduced.

1.2. Effects of Different Types of Solvent and Solvent Flowrate

Propane and CO_2 have high solubility with crude oil (Martin and Taber, 1992; Das and Butler, 1996; Badamchi-Zadeh et al., 2009; Coelho et al., 2015). However, propane has higher solubility with Peace River bitumen than CO_2 (Table D-2, Appendix D). Moreover, propane causes higher oil swelling factor (Yang and Gu, 2006). The swelling factor is the volume of the oil with dissolved gases divided by the volume of the gas-free oil (Simon and Graue, 1965).

For these reasons, propane-steam presented higher recovery than CO_2-steam for the sand-only rock. For the sand-clay rock, propane-steam and CO_2-steam had similar performances. It is believed that the reservoir clay-asphaltene interactions dampen the higher solubility of propane with crude oil.

Also, steam-flooding on clean-sand reservoir rock (E8) had higher oil recovery than SSF with clays (E6 and E7). This indicates that clays have greater influence on recovery performance than the type of solvent.

Moreover, the lowest solvent flowrate caused highest oil recovery and faster production for SSF. The main reasons for the better performance of low solvent flowrates are higher thermal efficiency, reduced viscous fingering, and lower asphaltene precipitation (Farouq Ali and Snyder, 1973; Redford, 1982; Hornbrook et al., 1991; Moreno-Arciniegas and Babadagli, 2014).

2. Rheology

The fluid viscosity and rheological behavior inside the reservoir are key parameters to the success of bitumen microscopic displacement (Haghighat and Maini, 2010; Ezeuko et al., 2013). These parameters are presented in this section for the produced oil samples from all 12 experiments.

The shear rate and shear stress of the original Peace River bitumen sample and the 12 produced oil samples were measured for torques ranging from 15 to 85%. The viscosities of the produced oil samples were measured from 30 to 80°C.

Rheological models have been tested on the shear stress *versus* shear rate data. The values for shear rate and shear stress were then fitted to a Power-Law Fluid Model with the following form (Ostwald and de Waele, 1923):

$$\tau = K \cdot \dot{\gamma}^{n} \quad (1)$$

where: τ – Shear stress

K – Flow consistency index

$\dot{\gamma}$ – Shear rate

n – Flow behavior index.

According to the value of the flow behavior index *n*, the fluids are classified as:

$n > 1$ – Shear Thickening

$n = 1$ – Newtonian

$n < 1$ – Shear Thinning.

The rheological modelling results are presented in Table B-1 (Appendix B). As the flow behavior index (*n*) is less than 1, all oil samples are shear-thinning. This rheological behavior is favorable to oil displacement as the internal friction reduces as shear rates increase, resulting in lower viscosities during oil mobilization (Green and Willhite, 1998).

The viscosity *versus* temperature curves, given in Figure 5, are regressed to a Power-Law function:

$$\mu = A \cdot T^{b} \tag{2}$$

where: μ – Viscosity

A – Constant (calculated by regression)

T – Temperature

b – Constant (calculated by regression).

The fitted Power-Law equations for the produced oil samples and their R^2 are presented in Table 4. Results from Table 4 were plotted in Figure 6, with the x-axis being $-b$ and the y-axis being A (constants from Eq. 2).

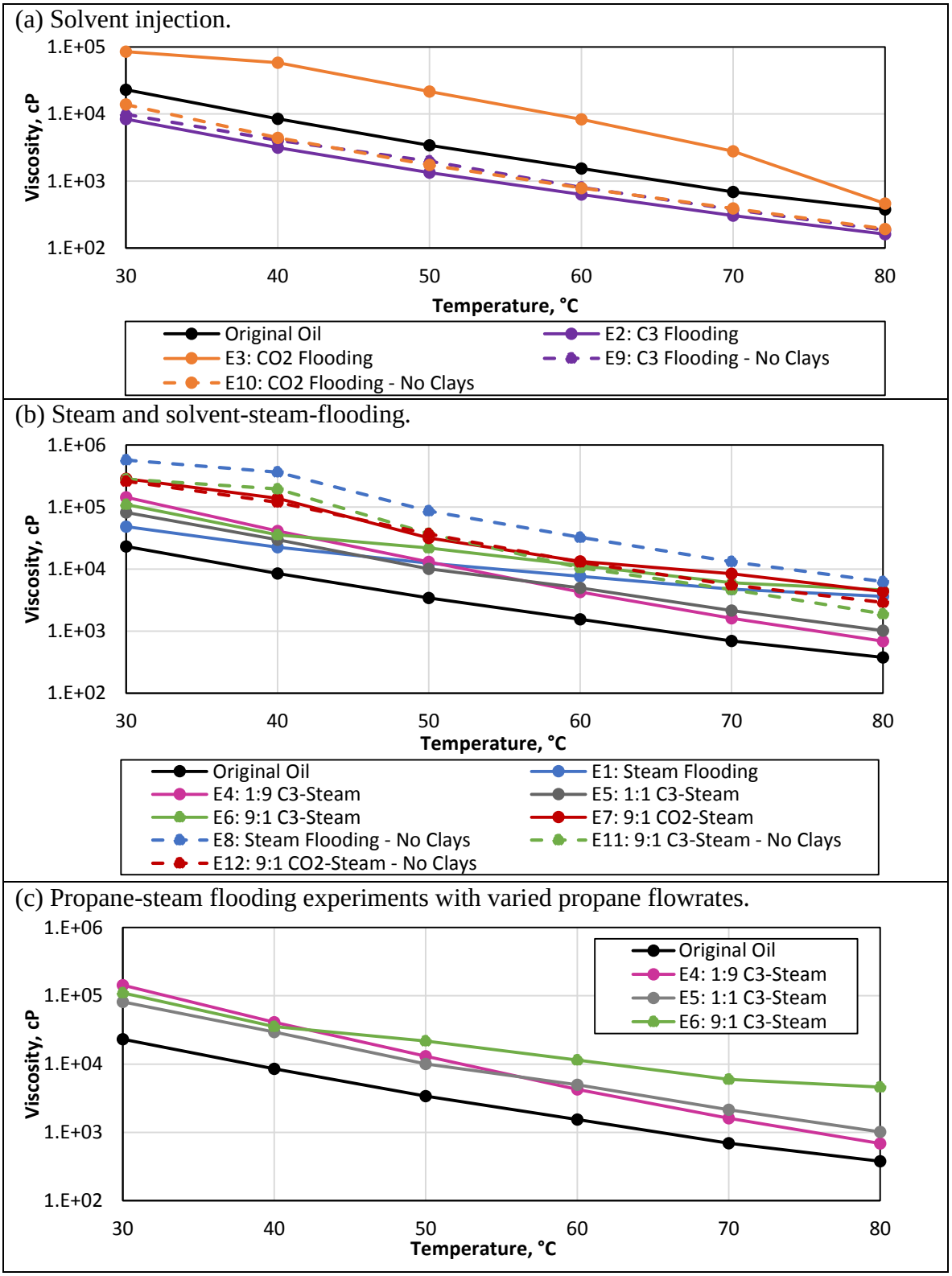

Figure 5. Produced oil viscosities as a function of temperature.

Table 4. Power-Law equations regressed for produced oil viscosities.

Oil Sample	Viscosity, cP (Power–Law Equation)	R^2
Original Oil	$\mu = 4.7E^{10} \cdot T^{-4.2}$	0.995
E1: Steam-flooding	$\mu = 4.3E^{8} \cdot T^{-2.7}$	0.999
E2: Propane Flooding	$\mu = 8.5E^{9} \cdot T^{-4.0}$	0.996
E3: CO_2 Flooding	$\mu = 5.7E^{12} \cdot T^{-5.1}$	0.893
E4: 1:9 Propane-Steam	$\mu = 2.2E^{13} \cdot T^{-5.5}$	0.994
E5: 1:1 Propane-Steam	$\mu = 3.7E^{11} \cdot T^{-4.5}$	0.994
E6: 9:1 Propane-Steam	$\mu = 6.3E^{9} \cdot T^{-3.2}$	0.993
E7: 9:1 CO_2-Steam	$\mu = 1.3E^{12} \cdot T^{-4.5}$	0.984
E8: Steam-flooding - No Clays	$\mu = 1.3E^{13} \cdot T^{-4.9}$	0.968
E9: Propane Flooding - No Clays	$\mu = 1.2E^{10} \cdot T^{-4.1}$	0.985
E10: CO_2 Flooding - No Clays	$\mu = 3.6E^{10} \cdot T^{-4.3}$	0.998
E11: 9:1 Propane-Steam - No Clays	$\mu = 4.9E^{13} \cdot T^{-5.4}$	0.960
E12: 9:1 CO_2-Steam - No Clays	$\mu = 3.9E^{12} \cdot T^{-4.8}$	0.985

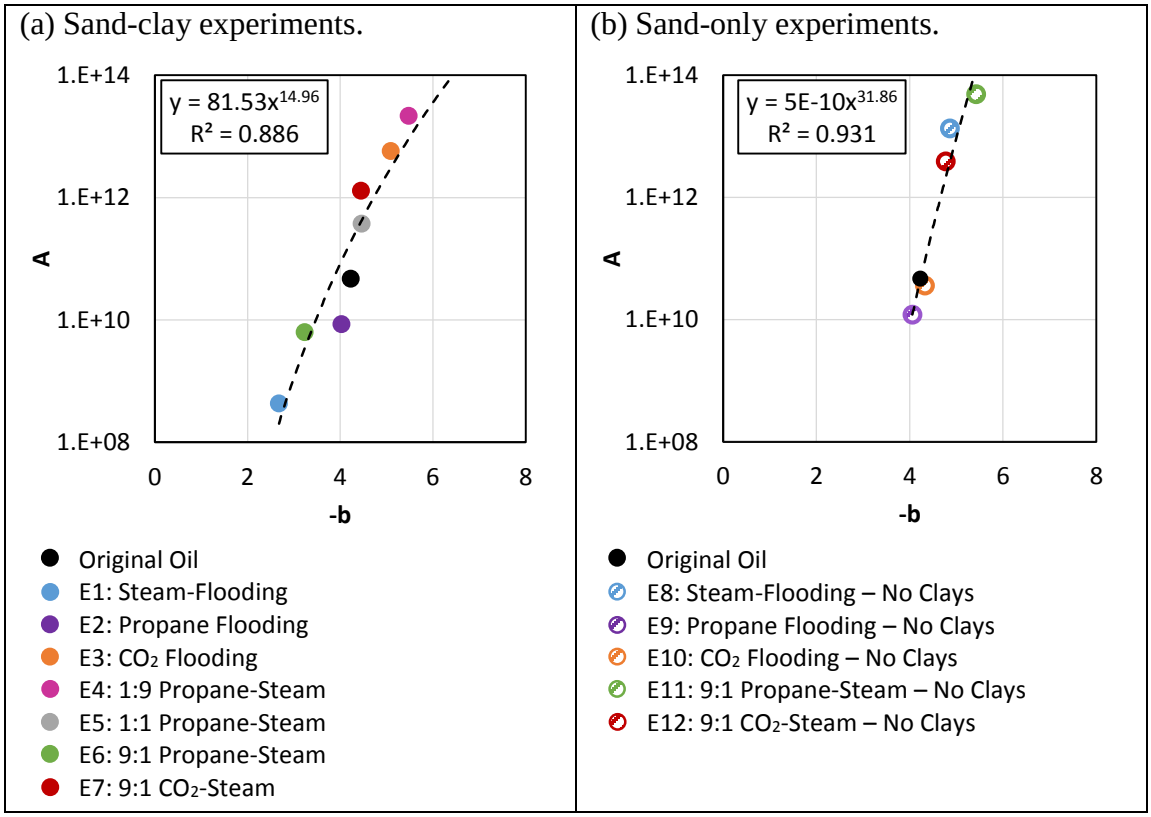

Figure 6. Relationship between Power-Law regression constants from Table 4. Dashed lines indicate trend lines.

For pure solvent flooding, only CO_2 flooding with clays (E3) produced more viscous oil than the original sample (Figure 5). For steam and SSF, all produced oil samples had higher viscosity than the original oil, regardless of the presence of clays or the solvent type.

Such high viscosities are also recognized in Figure 6, which shows that the produced oil samples displayed higher values for the Power Law constants *A* and *b* as compared to the original oil (except for E10). High values for *A* and *b* reflect in an increse in oil viscosity. It is believed that the presence of clays and stable water-in-oil emulsions are responsible for the alterations in the oil viscosity.

To further understand the role of clays in the rheological behavior of produced oil samples, the original bitumen was mixed with clays at different amounts (10 to 40 wt%). The viscosity of the four pseudo-mixtures were measured at 30 and 80°C. Results are presented in Figure 7. The values at 0 wt% represent the original bitumen viscosity at 30 and 80°C (black curves in Figure 5).

As the clay content in the original bitumen increases, the oil viscosity increases exponentially (Figure 7). Such behavior is explained by the formation of clay-asphaltene solids, which increase the friction within the oil phase. Therefore, the reason for the high viscosities obtained for solvent flooding is the clay content of the produced oil samples.

In addition to the presence of clays, previous works have observed that water-in-oil emulsions in the produced oil (Figure 4) also cause viscosities to increase (Rivero and Mamora, 2005; Alboudwarej, 2007; Ezeuko et al. 2013), which justifies the high viscosities observed for the steam and SSF samples.

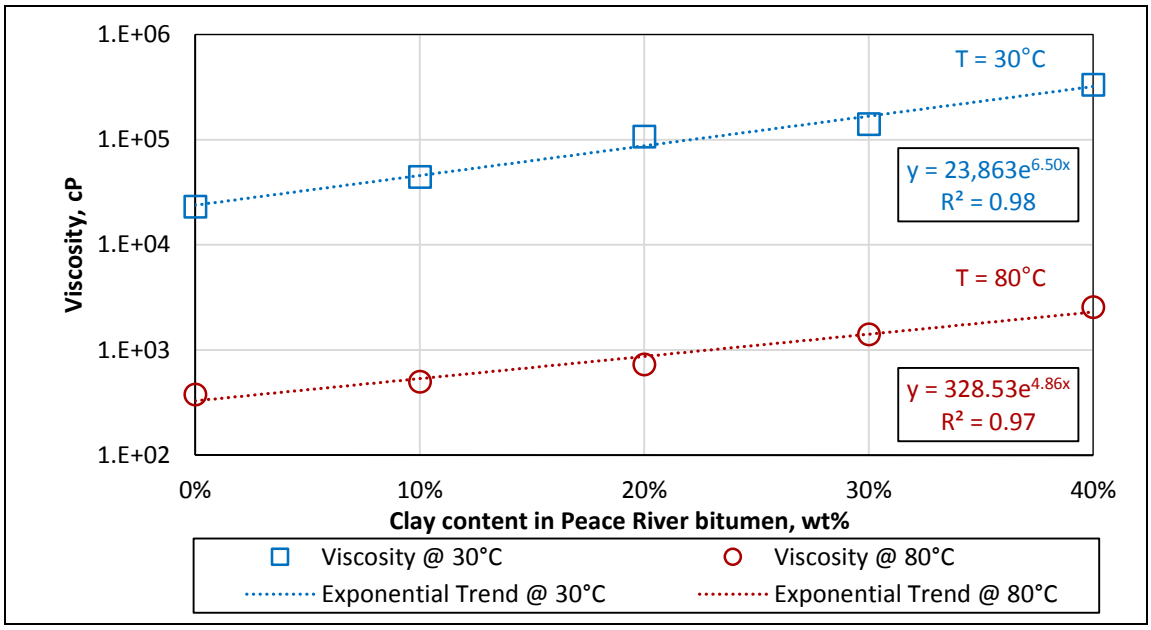

Figure 7. Effect of clays on Peace River bitumen viscosity.

3. Asphaltene, Clay, and Water Content

The asphaltene content in the produced oil is determined by using *n*-pentane dilution (ASTM, 2011), whereas the clay content is determined by washing and filtering the oil samples with toluene (Amyx et al., 1960; Kar and Hascakir, 2015). The water content was determined with TGA/DSC considering the mass loss at 150°C (Figures C-1 through C-3, Appendix C).

Asphaltenes are defined as the crude oil fractions which are soluble in aromatic solvents (e.g. toluene and benzene) and insoluble in normal alkanes such as propane (Mitchell and Speight, 1973; Speight, 2006). Asphaltenes are also insoluble in CO_2 (Mungan, 1981; Deo and Parra, 2012). However, the precipitated asphaltenes are

chemically and morphologically different for each injected solvent (Thawer et al., 1990; Monger and Trujillo, 1991; Butler and Mokrys, 1991; Deo and Parra, 2012).

Asphaltenes and clays are also known to stabilize emulsions due to their polarity (Sztukowski and Yarranton, 2005; Kokal, 2005; Kar et al., 2014).

Figure 8 presents the produced oil compositions in terms of water-in-oil emulsions, de-asphalted oil (DAO), asphaltenes, and clays. Figure 9 shows the asphaltene and DAO content of the produced oils, excluding the contribution of clays and water.

Results indicate a trade-off on the oil quality when clays are present: whilst asphaltene content and emulsions may reduce, clays migrate into the oil phase.

Moreover, the experiments with propane-steam produced higher quality oil, with lower asphaltene content than CO_2-Steam. Increasing propane flowrate caused higher asphaltene precipitation due to excess solvent, increasing oil quality.

The amount of water in the produced oil in the form of water-in-oil emulsions was higher for the experiments without clays, which is explained by the higher asphaltene content of those samples (Figures 8 and 9).

It was also found that SSF with propane or CO_2 reduces water-in-oil emulsions as compared to steam-flooding (Figure C-2a, Appendix C). Figures 8 and C-3a (Appendix C) indicate that higher solvent concentrations cause less water-in-oil emulsions. Moreover, propane and propane-steam injection presented less emulsions than when CO_2 was injected.

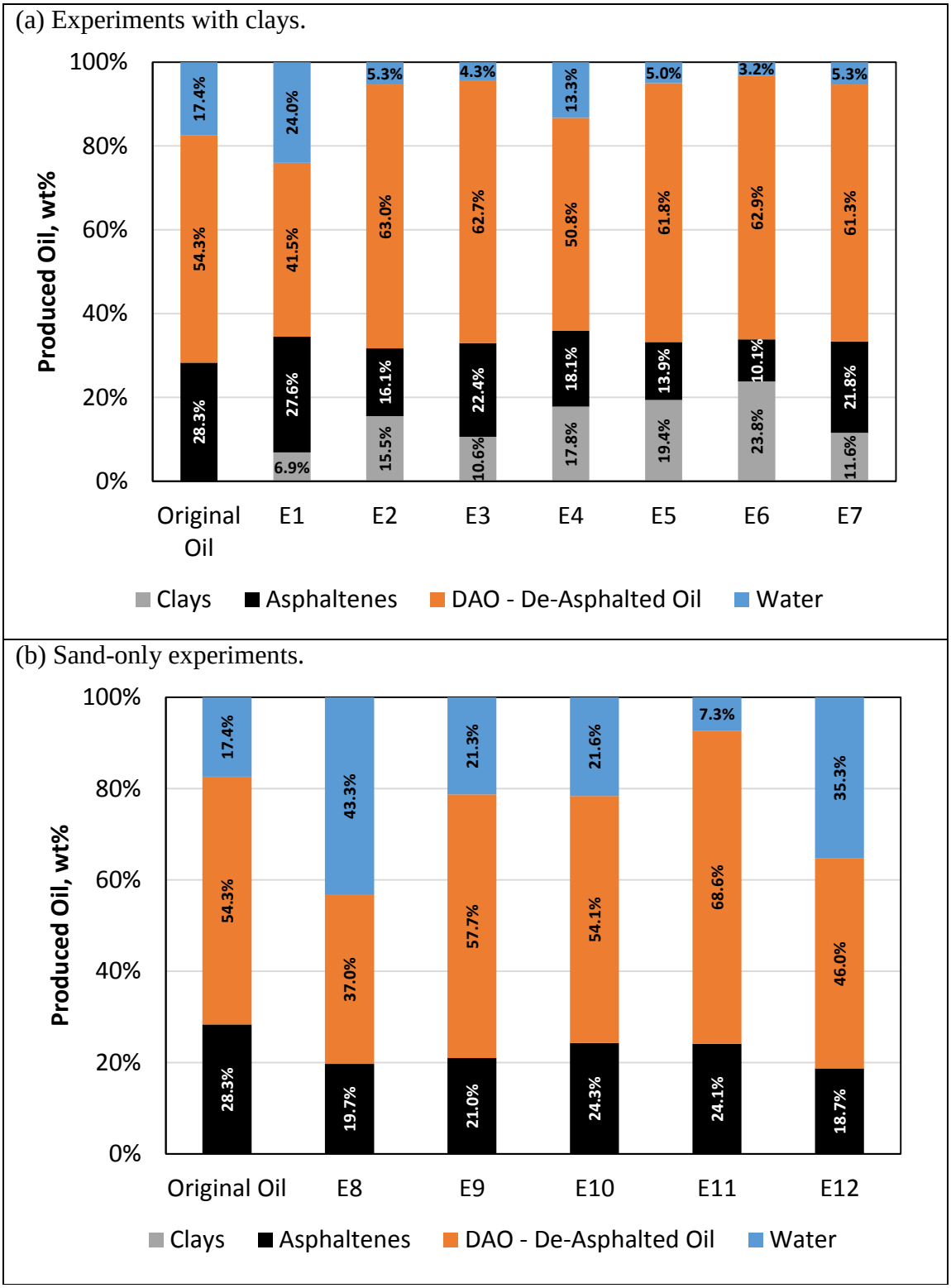

Figure 8. Produced oil composition, considering clays, asphaltenes, DAO, and water.

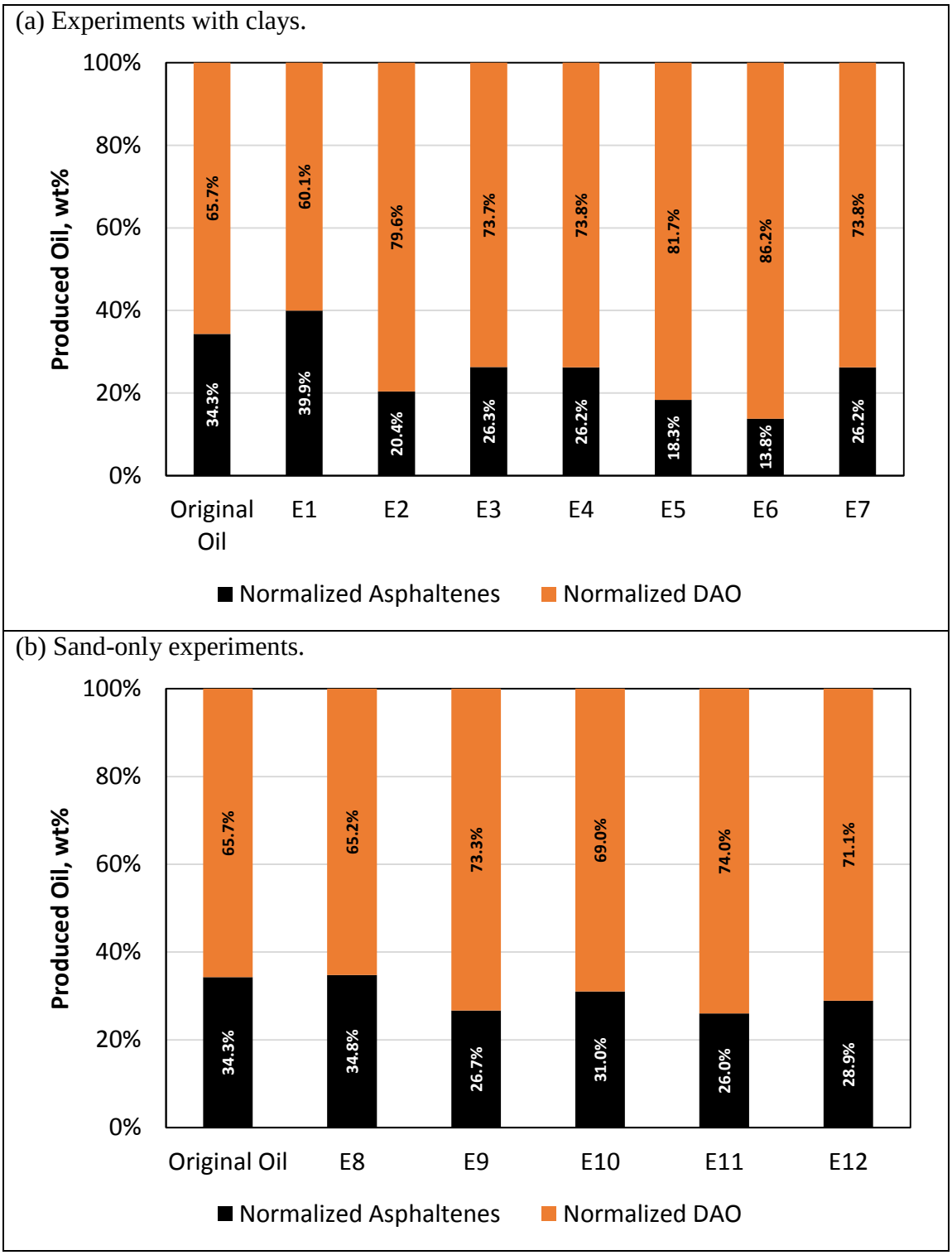

Figure 9. Normalized produced oil sample composition, considering only the presence of DAO and asphaltenes (water and clays excluded).

4. Spent-Rock Analysis

Figure 10 presents the pictures of the postmortem samples. In these pictures, the left-hand side shows the solvent and/or steam injection point, while the right-hand side is the production point. As it can be visualized, the inlet and outlet of the cores significantly varied in terms of color.

Therefore, all the spent-rock analyses were carried out using postmortem inlet and outlet samples. First, residual oil saturations were determined through TGA/DSC analysis (Figures C-5 through C-8, Appendix C). Then, the microscopic (pore-scale) sweep efficiency was calculated by using the following equation:

$$E_S = 1 - \frac{S_{or}}{S_{oi}} \tag{3}$$

where: E_S – Sweep efficiency

S_{or} – Residual oil saturation

S_{oi} – Initial oil saturation.

The initial oil saturations are 15.6 wt% (sand and clay rock) and 17.8 wt% (sand-only rock). Residual oil saturations results are reported in Table 5 and the calculated sweep efficiencies are presented in Table 6.

Clays had a double negative effect on the sweep efficiency by increasing residual oil and by reducing the sweep uniformity. On average, the cases with clays had 95.7% higher sweep efficiency on the production side than close to the injection, whilst without clays the sweep on the injection was just 12.9% higher.

E1: Steam Flooding	E2: Propane Flooding
	
E3: CO_2 Flooding	E4: 1:9 Propane-Steam
	
E5: 1:1 Propane-Steam	E6: 9:1 Propane-Steam
	
E7: 9:1 CO_2-Steam	E8: Steam Flooding - No Clays
	
E9: Propane Flooding - No Clays	E10: CO_2 Flooding - No Clays
	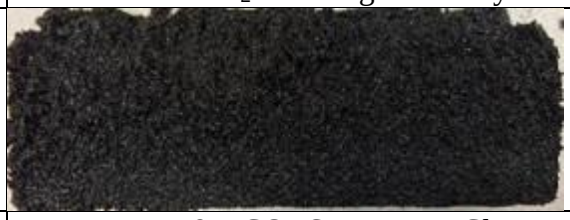
E11: 9:1 Propane-Steam - No Clays	E12: 9:1 CO_2-Steam - No Clays
	

Figure 10. Spent-rock pictures. Injection is from left to right.

Overall, propane displays higher sweep and uniformity than CO_2, relating to the higher solubility of propane with Peace River bitumen (Table D-2, Appendix D). Moreover, for SSF at varied propane flowrates, the lowest rate case displayed higher sweep efficiency and uniformity.

To investigate the residual oil left on the spent-rock, the residual oil was separated by using solvent dilution and filtration methods (Amyx et al., 1960; Kar and Hascakir, 2015). Then, the residual oil components are divided into asphaltenes, DAO, clays attached to DAO, and clays attached to asphaltenes (Figure 11).

Results indicate that the use of different solvents control both the residual oil composition (asphaltene and DAO content) and the amount of clays that get attached to each fraction.

The residual oil precipitates caused by solvent flooding were investigated using TGA/DSC by combusting samples under nitrogen injection up to 800˚C (Figure C-4, Appendix C).

Table 5. Residual oil saturations.

	S_{or} at cell inlet, wt%	**S_{or} at cell outlet, wt%**
E1: Steam-flooding	13.1%	7.3%
E2: Propane Flooding	11.6%	10.6%
E3: CO_2 Flooding	12.8%	10.4%
E4: 1:9 Propane-Steam	6.9%	4.0%
E5: 1:1 Propane-Steam	10.0%	5.4%
E6: 9:1 Propane-Steam	10.5%	7.0%
E7: 9:1 CO_2-Steam	12.1%	6.3%
E8: Steam-flooding - No Clays	3.2%	3.8%
E9: Propane Flooding - No Clays	2.8%	6.0%
E10: CO_2 Flooding - No Clays	2.6%	7.1%
E11: 9:1 Propane-Steam - No Clays	2.8%	3.2%
E12: 9:1 CO_2-Steam - No Clays	3.6%	3.3%

Results in Figures 11b and C-4 (Appendix C) indicate that CO_2 precipitates are lighter than propane precipitates. Such observations agree with the literature, which reported that CO_2 precipitates are rich in saturates and aromatics, while propane precipitates are richer in high molecular weight asphaltenes (Monger and Trujillo, 1991; Butler and Mokrys, 1991; Deo and Parra, 2011).

Table 6. Calculated microscopic sweep efficiency. Results obtained using Eq. 3.

	E_S at cell inlet, wt%	**E_S at cell outlet, wt%**
E1: Steam-flooding	15.8%	53.4%
E2: Propane Flooding	26.0%	32.3%
E3: CO_2 Flooding	17.7%	33.5%
E4: 1:9 Propane-Steam	55.6%	74.5%
E5: 1:1 Propane-Steam	35.8%	65.2%
E6: 9:1 Propane-Steam	32.8%	55.0%
E7: 9:1 CO_2-Steam	22.6%	59.4%
E8: Steam-flooding - No Clays	82.8%	78.4%
E9: Propane Flooding - No Clays	84.4%	66.5%
E10: CO_2 Flooding - No Clays	85.6%	60.2%
E11: 9:1 Propane-Steam - No Clays	84.4%	82.3%
E12: 9:1 CO_2-Steam - No Clays	80.0%	81.7%

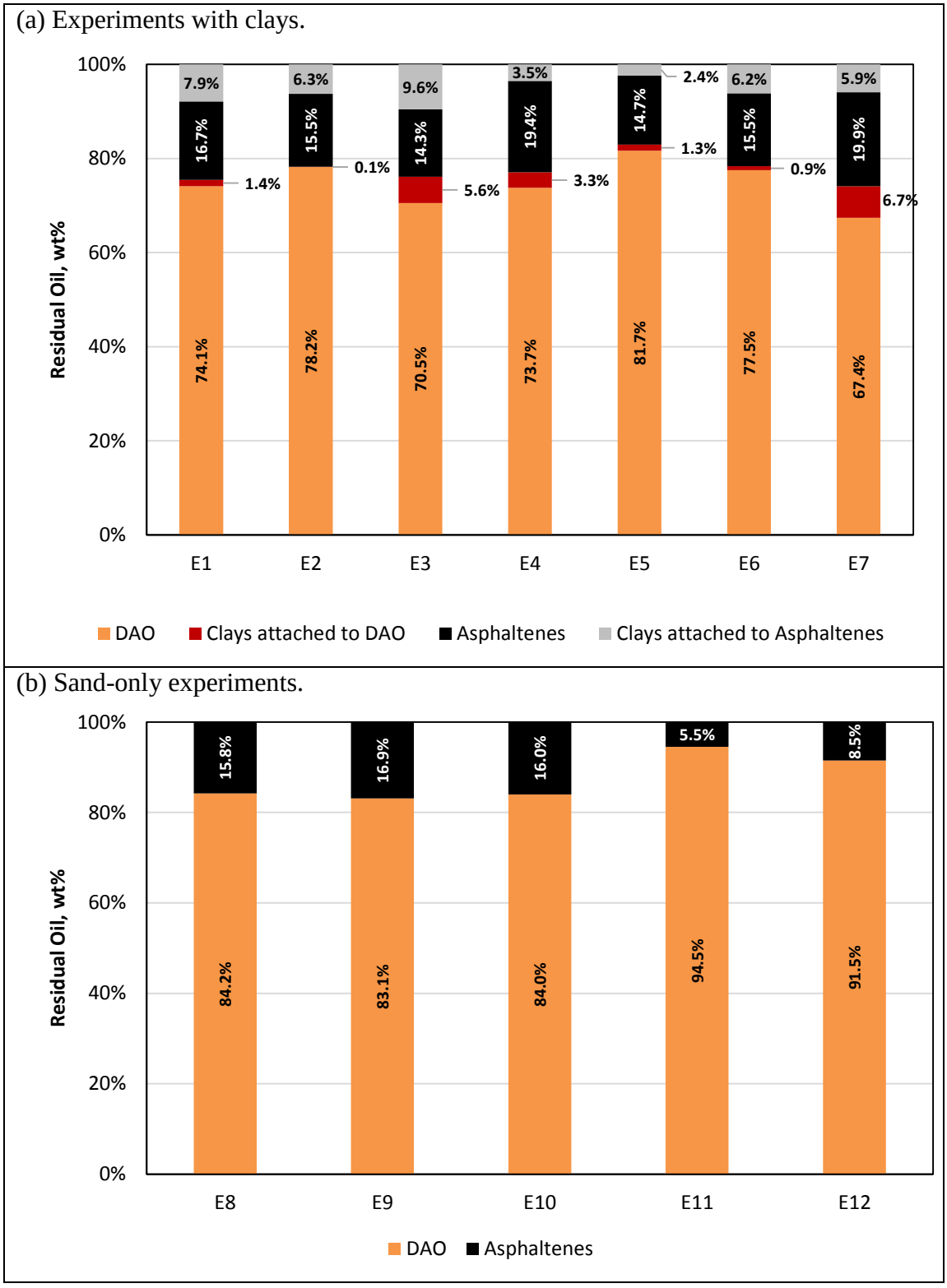

Figure 11. Residual oil composition, including clays.

2. Upscaling Considerations

Regarding the main microscopic phenomena controlling bitumen extraction, the solvent-water-crude phase behavior and gravity segregation are considered the most sensitive parameters for upscaling results.

Though steam-flooding causes both solvents to be immiscible with Peace River oil, at field pressures the solvent solubilities with bitumen are estimated to be up to 20 times higher than in the experiments (Table D-2, Appendix D), which may be further improved by the gas in solution (Firoozabadi, 2001).

Therefore, the higher solvent-crude interactions would have to be taken into account for upscaling the recovery performance results. Additionally, at higher pressures, the solubility of CO_2 and propane to water is also altered (Wiebe and Gaddy, 1940; Kobayashi and Katz, 1953, Hangx, 2005).

Moreover, the higher pressure, temperature, and solvent solubilities would alter the asphaltene precipitation behavior (Speight et al., 1984).

Gravity segregation must also be taken in consideration as the experimental setup simulates piston-like displacement by vertical, 1-D fluid injection. In the reservoir, however, steam and solvent gravity override is expected to control the recovery efficiency (Green and Willhite, 1998; Speight, 2009; Vannaxay et al., 2014).

Other studies also demonstrate that the oil composition, geology, reservoir properties, and fluid injection strategies also control the effectiveness of SSF (Redford, 1982; Gumrah and Bagci, 1997; Demiral et al., 2003; Vannaxay et al., 2014). Thus, such characteristics should be carefully examined for each potential field application.

CHAPTER IV

CONCLUSIONS

12 core flooding experiments were performed to investigate the microscopic displacement mechanisms controlling Peace River bitumen extraction during solvent, steam, and solvent-steam-flooding. The oil recovery performance, produced oil quality, residual oil quality, and sweep efficiency of each experiment were evaluated for different types of reservoir rocks (with and without clays) and solvents (propane and CO_2).

It was found that reservoir fines (clays) dramatically reduce the microscopic displacement efficiency of bitumen. By impairing permeability and porosity, the clays decrease sweep efficiency and cause more viscous fingering. Consequently, when clays were present, bitumen recovery was reduced and the oil production was delayed.

Clay-asphaltene interactions posed a trade-off to the produced oil quality: whereas some asphaltene fractions are removed from the oil and water-in-oil emulsions are reduced, clays dispersed within the oil cause the viscosity to increase exponentially.

The addition of propane and CO_2 to steam-flooding increased recoveries and expedited oil production. It was found that propane has higher solubility with bitumen and causes more asphaltene precipitation than CO_2. These effects allow better sweep efficiency for the hydrocarbon solvent. However, such effects were dampened when clays were present, causing propane–steam and CO_2–steam to yield similar oil recoveries. The presence of clays was also recognized to be more prejudicial when propane was used.

Overall, no oil upgrading was observed for propane–steam or CO_2–steam due to the formation of emulsions and clay migration. However, propane produced lighter oils than CO_2.

Lower solvent flowrates were also recognized to yield higher sweep efficiency and recovery, as well as to produce lighter oil. An optimum solvent injection can be devised to maximize solubilization before breakthrough, while minimizing formation damage.

Ultimately, the experimental studies allowed the understanding that bitumen extraction performance during solvent-steam is highly controlled by the microscopic recovery efficiency.

REFERENCES

Alboudwarej, H., Felix, J., Taylor, S. et al. 2006. Highlighting Heavy Oil. *Oilfield Review* **18** (2): 34–53.

Alboudwarej, H., Muhammad, M., Shahraki, A. K., Dubey, S., Vreenegoor, L., and Saleh, J. M. 2007. Rheology of Heavy-Oil Emulsions. *SPE Prod Oper* **22** (3): 285–293. SPE-97886-PA. http://dx.doi.org/10.2118/97886-PA.

Amyx, J. W., Bass, D. M., and Whiting, R. L. 1960. *Petroleum Reservoir Engineering, Physical Properties*. New York, New York: McGraw-Hill College.

API. 1980. *Manual of Petroleum Measurement Standards*. American Petroleum Institute. Available online at http://goo.gl/uv6KyA (Accessed 2/10/2016).

ASTM. 2011. *ASTM D2007-11: Standard Test Method for Characteristic Groups in Rubber Extender and Processing Oils and Other Petroleum-Derived Oils by the Clay-Gel Absorption Chromatographic Method*. West Conshohocken, Pennsylvania: ASTM International. http://dx.doi.org/10.1520/D2007-11.

Bachu, S. 2016. Identification of Oil Reservoirs Suitable for CO_2-EOR and CO_2 Storage (CCUS) Using Reserves Databases, with Application to Alberta, Canada. *Int J Greenh Gas Con* **44** (2016): 152–165. http://goo.gl/t2SfkG.

Bachu, S. and Stewart, S. 2002. Geological Sequestration of Anthropogenic Carbon Dioxide in the Western Canada Sedimentary Basin: Suitability Analysis. *J Can Pet Technol* **41** (2): 32–40. PETSOC-02-02-01. http://dx.doi.org/10.2118/02-02-01.

Badamchi-Zadeh, A., Yarranton, H. W., Maini, B. B., and Satyro, M. A. 2009. Phase Behavior and Physical Property Measurements for VAPEX Solvents: Part II. Propane, Carbon Dioxide and Athabasca Bitumen. *J Can Pet Technol* **48** (3): 57–65. PETSOC-09-03-57. http://dx.doi.org/10.2118/09-03-57.

Bayliss, P. and Levinson, A.A. 1976. Mineralogical Review of the Alberta Oil Sand Deposits (Lower Cretaceous, Mannville Group). *B Can Petrol Geol*, **24** (2): 211–224.

Bil, K. J., De Waal, J. A., Dicker, A. I. M., and Kantorowicz, J. D. 1988. Petrophysical Core Analysis of Sandstones Containing Delicate Illite. *Log Anal* **29** (5): 317–331. SPWLA-1988-v29n5a1.

Butler, R. M. and Mokrys, I. J. 1991. A New Process (VAPEX) for Recovering Heavy Oils Using Hot Water and Hydrocarbon Vapour. *J Can Pet Technol* **48** (3): 57–65. PETSOC-91-01-09. http://dx.doi.org/10.2118/91-01-09.

Bybee, K. 2008. The CO_2 Pilot at Lacq: An Integrated Oxycombustion CO_2-Capture and -Storage Project. *J Pet Technol* **60** (7): 90–91. SPE-0708-0090-JPT. http://dx.doi.org/10.2118/0708-0090-JPT.

Carson, P. A. and Mumford, C. 2002. *Hazardous Chemicals Handbook*. Woburn, MA: Elsevier Science.

Coelho, R. and Hascakir, B. 2015. The Pore-Scale Description of Carbon Dioxide Storage into High Asphaltene Content Reservoirs. Presented at the Carbon Management Technology Conference, 17-19 November, Sugar Land, Texas, USA. CMTC-439523-MS. http://dx.doi.org/10.7122/439523-MS.

Coelho, R., Barrufet, M., and Hascakir, B. 2015. Effect of Impurities in Carbon Dioxide Stream on Phase Behavior for Geological Storage of Carbon Dioxide in Low API Gravity Oil Reservoirs. Presented at the Carbon Management Technology Conference, 17-19 November, Sugar Land, Texas, USA. CMTC-439524-MS. http://dx.doi.org/10.7122/439524-MS.

Das, S. K. and Butler, R. M. 1996. Diffusion Coefficients of Propane and Butane in Peace River Bitumen. *Can J Chem Eng* **74** (6): 985–992. http://goo.gl/piIGzj.

Demiral, B. M. R., Gumrah, F., and Okandan, E. 2003. Tracking of Three-Phase Fluid Saturation by Computerized Tomography during Steam-CO_2 Injection. Presented at the Canadian International Petroleum Conference, 10-12 June, Calgary, Alberta. PETSOC-2003-216. http://dx.doi.org/10.2118/2003-216.

Deo, M. and Parra, M. 2012. Characterization of Carbon-Dioxide-Induced Asphaltene Precipitation. *Energy & Fuels* **26** (5): 2672–2679. http://goo.gl/1dHS5q.

ECCC. 2013. Canada's Emissions Trends. Report by Environmental and Climate Change Canada. Available online at https://goo.gl/JZQcqj (Accessed at 20/12/2015).

EIA. 2015. Annual Energy Outlook 2015 with Projections to 2040. Report by United States Energy Information Administration, Washington.

ExxonMobil. 2013. The Outlook for Energy: A View to 2040. *ExxonMobil* **6**.

Ezeuko, C. C., Wang, J., and Gates, I. D. 2013. Investigation of Emulsion Flow in Steam-Assisted Gravity Drainage. *SPE J* **18** (3): 440–447. SPE-157830-PA. http://dx.doi.org/10.2118/157830-PA.

Farouq Ali, S. M. and Abad, B. 1976. Bitumen Recovery from Oil Sands, Using Solvents in Conjunction with Steam. *J Can Pet Technol* **15** (3): 80–90. PETSOC-76-03-11. http://dx.doi.org/10.2118/76-03-11.

Farouq Ali, S. M. and Snyder, S. G. 1973. Miscible Thermal Methods Applied to a Two-Dimensional, Vertical Tar Sand Pack, with Restricted Fluid Entry. *J Can Pet Technol* **12** (4): 20–26. PETSOC-73-04-01. http://dx.doi.org/10.2118/73-04-01.

Firoozabadi, A. 2001. Mechanisms of Solution Gas Drive in Heavy Oil Reservoirs. *J Can Pet Technol* **40** (3): 15–20. PETSOC-01-03-DAS. http://dx.doi.org/10.2118/01-03-DAS.

Frauenfeld, T. W., Jossy, C., Bleile, J., Krispin, D., and Ivory, J. 2009. Experimental and Economic Analysis of the Thermal Solvent and Hybrid Solvent Processes. *J Can Pet Technol* **48** (11): 55–62. SPE-130445-PA. http://dx.doi.org/10.2118/130445-PA.

Goobie, G. and Kelly, S. 2012. Western Canadian Propane, Heavy Oil and Diluent Supply and Demand. Report by IHS. Available online at https://goo.gl/Njd2vz (Accessed on 12/19/2015).

Green, D.W. and Willhite, G.P. 1998. *Enhanced Oil Recovery*, SPE Textbook Series. Richardson, Texas: Society of Petroleum Engineers.

Gumrah, F. and Bagci, S. 1997. Steam-CO_2 Drive Experiments Using Horizontal and Vertical Wells. *J Petrol Sci Eng*, **18** (1): 113–129. http://goo.gl/4XCg7U.

Haghighat, P. and Maini, B.B. 2010. Role of Asphaltene Precipitation in VAPEX Process. *J Can Pet Technol* **49** (3): 14–21. SPE-134244-PA. http://goo.gl/SHIq0o.

Hajiw, M., Chapoy, A., and Coquelet, C. 2015. Hydrocarbons–Water Phase Equilibria Using the CPA Equation of State with a Group Contribution Method. *Can J Chem Eng* **93** (2): 432–442. http://dx.doi.org/10.1002/cjce.22093.

Hamm, R.A. and Ong, T.S. 1995. Enhanced Steam-Assisted Gravity Drainage: A New Horizontal Well Recovery Process for Peace River, Canada. *J Can Pet Technol* **34** (4): 33–40. PETSOC-95-04-03. http://dx.doi.org/10.2118/95-04-03.

Hangx, S. J. T. 2005. Behaviour of the CO_2-H_2O System and Preliminary Mineralisation Model and Experiments. *CATO J* **4** (1): 1–43.

Hein, F. J. and Marsh, R. A. 2008. Regional Geologic Framework, Depositional Models and Resource Estimates of the Oil Sands of Alberta, Canada. Presented at the World Heavy Oil Congress, 10–12 March, Edmonton, Canada. ETDEWEB ID: 21025370.

Hernandez, O. E. and Farouq Ali, S. M. 1972. Oil Recovery from Athabasca Tar Sand by Miscible-Thermal Methods. Presented at the Annual Technical Meeting, May 16-19, Calgary, Alberta. PETSOC-7249. http://dx.doi.org/10.2118/7249.

Hitchon, B. 1963. Geochemical Studies of Natural Gas Part I. Hydrocarbons in Western Canadian Natural Gases. *J Can Pet Technol* **2** (2): 60–76. PETSOC-63-02-05. http://dx.doi.org/10.2118/63-02-05.

Hornbrook, M. W., Dehghani, K., Qadeer, S., Ostermann, R. D., and Ogbe, D. O. 1991. Effects of CO_2 Addition to Steam on Recovery of West Sak Crude Oil. *SPE Reservoir Eng* **6** (3): 278–286. SPE-18753-PA. http://dx.doi.org/10.2118/18753-PA.

Huc, A. Y. 2011. *Heavy Crude Oils. From Geology to Upgrading: An Overview*. Paris: Editions Technip.

Hughes, C.R., Davey, R.C., and Curtis, C.D. 1989. Chemical Reactivity of Some Reservoir Illites: Implications for Petroleum Production. *Clay Minerals* **24** (2): 445–458.

IHS. 2012. Recent Developments in International Supply and Demand of Propane. NPGA 2012 Winter Board of Directors Meeting. Presentation. Available online at https://goo.gl/bdx8x6 (Accessed on 19/12/2015).

Juanes, R., Spiteri, E.J., Orr Jr., F.M., and Blunt, M.J. 2006. Impact of Relative Permeability Hysteresis on Geological CO_2 Storage. *Water Resour Res* **42** (12): 21–13. W12418. http://dx.doi.org/10.1029/2005WR004806.

Kar, T. and Hascakir, B. 2015. The Role of Resins, Asphaltenes and Water in Water-Oil Emulsion Breaking with Microwave Heating. *Energy & Fuels* **29** (6): 3684–3690. http://dx.doi.org/10.1021/acs.energyfuels.5b00662.

Kar, T., Mukhametshina, A., Unal, Y., and Hascakir, B. 2015. The Effect of Clay Type on Steam-Assisted-Gravity-Drainage Performance. *J Can Pet Technol* **54** (6): 412–423. SPE-173795-PA. http://dx.doi.org/10.2118/173795-PA.

Kar, T., Williamson, M., and Hascakir, B. 2014. The Role of Asphaltenes in Emulsion Formation for Steam Assisted Gravity Drainage (SAGD) and Expanding Solvent - SAGD (ES-SAGD). Presented at the SPE Heavy and Extra Heavy Oil Conference: Latin America, 24-26 September, Medellín, Colombia. SPE-171076-MS. http://dx.doi.org/10.2118/171076-MS.

Keshavarz, M., Okuno, R., and Babadagli, T. 2015. Optimal Application Conditions for Steam/Solvent Coinjection. *SPE Reserv Eval Eng* **18** (1): 20–38. SPE-165471-PA. http://dx.doi.org/10.2118/165471-PA.

Klock, K. and Hascakir, B. 2015. Simplified Reaction Kinetics Model for In-Situ Combustion. Presented at the SPE Latin American and Caribbean Petroleum Engineering Conference, 18-20 November, Quito, Ecuador. SPE-177134-MS. http://dx.doi.org/10.2118/177134-MS.

Kobayashi, R. and Katz, D. 1953. Vapor-Liquid Equilibria for Binary Hydrocarbon-Water Systems. *Ind Eng Chem* **45** (2): 440–446. http://dx.doi.org/10.1021/ie50518a051.

Kokal, S. L. 2005. Crude Oil Emulsions: A State-Of-The-Art Review. *SPE Prod Facil* **20** (1): 5–13. SPE-77497-PA. http://dx.doi.org/10.2118/77497-PA.

Kontogeorgis, G. M., Voutsas, E. C., Yakoumis, I. V., and Tassios, D. P. 1996. An Equation of State for Associating Fluids. *Ind Eng Chem* **35** (11): 4310–4318. http://dx.doi.org/10.1021/ie9600203.

Leontaritis, K., Amaefule and J., Charles, R.E. 1994. A Systematic Approach for the Prevention and Treatment of Formation Damage Caused by Asphaltene Deposition. S*PE Prod Facil* **9** (3): 157–164. SPE-23810-PA. http://dx.doi.org/10.2118/23810-PA.

Li, H., Zheng, S. and Yang, D., 2013. Enhanced Swelling Effect and Viscosity Reduction of Solvent(s)/CO_2/Heavy-Oil Systems. *SPE J* **18** (4): 695–707. PE-150168-PA. http://dx.doi.org/10.2118/150168-PA.

Li, W. and Mamora, D.D. 2010. Drainage Mechanism of Steam with Solvent Coinjection under Steam Assisted Gravity Drainage (SAGD) Process. Presented at the International Oil and Gas Conference and Exhibition in China, 8-10 June, Beijing, China. SPE-130802-MS. http://dx.doi.org/10.2118/130802-MS.

Marchal, V., Dellink, R., Van Vuuren, D., Clapp, C., Chateau, J., Magné, B. and van Vliet, J. 2011. OECD Environmental Outlook to 2050. In *Organization for Economic Co-operation and Development. Climate Change - Chapter 3*. Pre-Release Version. Available online at http://www.oecd.org/env/cc/49082173.pdf (Accessed in 28/10/2015)

Martin, D. F. and Taber, J. J. 1992. Carbon Dioxide Flooding. *J Pet Technol* **44** (4): 396–400. SPE-23564-PA. http://dx.doi.org/10.2118/23564-PA.

McCain, W.D. 1990. *Properties of Petroleum Fluids*. Tulsa, Oklahoma: Pennwell Books.

Metz, B., Davidson, O., Coninck, H.D., Loos, M., and Meyer, L. 2005. *IPCC Special Report on Carbon Dioxide Capture and Storage*. Cambridge, UK: Cambridge University Press.

Mitchell, D.L. and Speight, J.G. 1973. The Solubility of Asphaltenes in Hydrocarbon Solvents. *Fuel* **52** (2): 149–152. http://dx.doi.org/10.1016/0016-2361(73)90040-9.

Mohammadzadeh, O., Rezaei, N., and Chatzis, I. 2010. Pore-Level Investigation of Heavy Oil and Bitumen Recovery Using Solvent−Aided Steam Assisted Gravity Drainage (SA-SAGD) Process. *Energy & Fuels* **24** (12): 6327–6345. http://dx.doi.org/10.1021/ef100621s.

Mohammed, M. A. and Babadagli, T. 2015. Efficiency of Steam-Over-Solvent-Injection-in-Fractured-Reservoirs (SOS-FR) Method Considering Oil Recovery and Solvent Retrieval: Core-Scale Experimentation. *J Can Pet Technol* **54** (5): 310–332. SPE-165528-PA. http://dx.doi.org/10.2118/165528-PA.

Monger, T. G. and Trujillo, D. E. 1991. Organic Deposition during CO_2 and Rich-Gas Flooding. *SPE Reservoir Eng* **6** (1): 17–24. SPE-18063-PA. http://goo.gl/RgHp4y.

Moreno-Arciniegas, L. and Babadagli, T. 2014. Optimal Application Conditions of Solvent Injection into Oil Sands to Minimize the Effect of Asphaltene Deposition: An Experimental Investigation. *SPE Reserv Eval Eng* **17** (4): 530–546. SPE-165531-PA. http://dx.doi.org/10.2118/165531-PA.

Mukhametshina, A., Kar, T. and Hascakir, B. 2015. Asphaltene Precipitation during Bitumen Extraction with Expanding-Solvent Steam-Assisted Gravity Drainage: Effects on Pore-Scale Displacement. *SPE J*. Preprint. SPE-170013-PA. http://dx.doi.org/10.2118/170013-PA.

Mungan, N. 1981. Carbon Dioxide Flooding-Fundamentals. *J Can Pet Technol* **20** (1): 87–92. PETSOC-81-01-03. http://dx.doi.org/10.2118/81-01-03.

Naderi, K. and Babadagli, T. 2014. Experimental Analysis of Heavy-Oil Recovery by Alternate Injection of Steam and Solvent (Hydrocarbon/CO_2) in Unconsolidated Sand Reservoirs. *J Can Pet Technol* **53** (5): 263–274. SPE-146738-PA. http://dx.doi.org/10.2118/146738-PA.

NASDAQ. 2016. End of day Commodity Futures Price Quotes for Crude Oil WTI (NYMEX). Report. Available online at http://goo.gl/h83A6l (Accessed 1/21/2016).

Nasr, T. N., Prowse, D. R., and Frauenfeld, T. 1987. The Use of Flue Gas with Steam in Bitumen Recovery from Oil Sands. *J Can Pet Technol* **26** (3): 62–69. PETSOC-87-03-06. http://dx.doi.org/10.2118/87-03-06.

Neasham, J. W. 1977. The Morphology of Dispersed Clay in Sandstone Reservoirs and Its Effect on Sandstone Shaliness, Pore Space and Fluid Flow Properties. Presented

at the SPE Annual Fall Technical Conference and Exhibition, 9-12 October, Denver, Colorado. SPE-6858-MS. http://dx.doi.org/10.2118/6858-MS.

Nghiem, L.X. and Coombe, D.A. 1997. Modeling Asphaltene Precipitation during Primary Depletion. *SPE J* **2** (2): 170–176. SPE-36106-PA. http://goo.gl/rcruqW.

NIOSH - National Institute for Occupational Safety and Health. 1976. Criteria for a Recommended Standard, Occupational Exposure to Carbon Dioxide. Report. Available online at http://goo.gl/ni571d (Accessed 1/7/2016).

Ordorica-Garcia, G., Nikoo, M., Carbo, M., and Bolea, I. 2012. Technology Options and Integration Concepts for Implementing CO_2 Capture in Oil-Sands Operations. *J Can Pet Technol* **51** (5): 362–375. SPE-137808-PA. http://goo.gl/zuHUw4.

Ostwald, W. and de Waele, A. 1923. Viscometry and Plastometry. *J Oil Colour Chem As* **6**: 33–69.

Pedersen, K.S., Christensen, P.L. and Shaikh, J.A. 2006. *Phase Behavior of Petroleum Reservoir Fluids*. Boca Raton, Florida: CRC Press.

Peneloux, A., Rauzy, E. and Fréze, R. 1982. A Consistent Correction for Redlich-Kwong-Soave Volumes. *Fluid Phase Equilibr* **8** (1): 7–23. http://dx.doi.org/10.1016/0378-3812(82)80002-2.

Pentland, C.H., El-Maghraby, R., Georgiadis, A., Iglauer, S. and Blunt, M.J. 2011. Immiscible Displacements and Capillary Trapping in CO_2 Storage. *Energy Procedia* **4**: 4969–4976. http://dx.doi.org/10.1016/j.egypro.2011.02.467.

Prats, M. 1982. *Thermal Recovery*. New York: H.L. Doherty Memorial Fund of AIME, Society of Petroleum Engineering of AIME.

Pruess, K., Xu, T., Apps, J., and Garcia, J. 2003. Numerical Modeling of Aquifer Disposal of CO_2. *SPE J* **8** (1): 49–60. SPE-83695-PA. http://dx.doi.org/10.2118/83695-PA.

Redford, D. A. 1982. The Use of Solvents and Gases with Steam in the Recovery of Bitumen from Oil Sands. *J Can Pet Technol* **21** (5): 45–53. PETSOC-82-01-03. http://dx.doi.org/10.2118/82-01-03.

Redford, D. A. and McKay, A. S. 1980. Hydrocarbon-Steam Processes for Recovery of Bitumen from Oil Sands. Presented at the SPE/DOE Enhanced Oil Recovery Symposium, 20-23 April, Tulsa, Oklahoma. SPE-8823-MS. http://goo.gl/AiwvRF.

Rivero, J. A. and Mamora, D. D. 2005. Production Acceleration and Injectivity Enhancement Using Steam-Propane Injection for Hamaca Extra-Heavy Oil. *J Can Pet Technol* **44** (2): 50–57. PETSOC-05-02-05. http://goo.gl/5KFT7l.

Scheflan, L. and Jacobs, M. B. 1953, *The Handbook of Solvents*. New York: D. Vas Nostrand Company, Inc.

Shaw, J. and Bachu, S. 2003. Evaluation of the CO_2 Sequestration Capacity in Alberta's Oil and Gas Reservoirs at Depletion and the Effect of Underlying Aquifers. *J Can Pet Technol* **42** (9): 51–61. PETSOC-03-09-02. http://dx.doi.org/10.2118/03-09-02.

Shu, W. R. and Hartman, K. J. 1988. Effect of Solvent on Seam Recovery of Heavy Oil. *SPE Reservoir Eng* **3** (2): 457−465. SPE-14223-PA. http://goo.gl/ktlFRI.

Simon, R. and Graue, D. J. 1965. Generalized Correlations for Predicting Solubility, Swelling and Viscosity Behavior of CO2-Crude Oil Systems. *J Pet Technol* **17** (1): 102–106. SPE-917-PA. http://dx.doi.org/10.2118/917-PA.

Smith, D. G., Hubbard, S. M., Leckie, D. A. and Fustic, M. 2009. Counter Point Bar Deposits: Lithofacies and Reservoir Significance in the Meandering Modern Peace River and Ancient McMurray Formation, Alberta, Canada. *Sedimentology* **56** (6): 1655−1669. http://dx.doi.org/10.1111/j.1365-3091.2009.01050.x.

Speight J.G. 2006. *The Chemistry and Technology of Petroleum*. New York, New York: CRC Press.

Speight, J. G. 2009. *Enhanced Recovery Methods for Heavy Oil and Tar Sands*. Houston, Texas: Gulf Publishing Company.

Speight, J. G., Long, R. B. and Trowbridge, T. D. 1984. Factors Influencing the Separation of Asphaltenes from Heavy Petroleum Feedstocks. *Fuel* **63** (5): 616−620. http://dx.doi.org/10.1016/0016-2361(84)90156-x.

Stone, T. and Ivory, J. 1987. An Examination of Steam-CO_2 Processes. *J Can Pet Technol* **26** (3): 54–61. PETSOC-87-03-08. http://dx.doi.org/10.2118/87-03-08.

Stone, T. and Malcolm, J. D. 1985. Simulation of a Large Steam-CO_2 Co-Injection Experiment. *J Can Pet Technol* **24** (6): 51–59. PETSOC-85-06-04. http://dx.doi.org/10.2118/85-06-04.

Svrcek, W. Y. and Mehrotra, A. K. 1989. Properties of Peace River Bitumen Saturated with Field Gas Mixtures. *J Can Pet Technol* **28** (2): 50–56. PETSOC-89-02-01. http://dx.doi.org/10.2118/89-02-01.

Sztukowski, D.M. and Yarranton, H.W. 2005. Oilfield Solids and Water-in-Oil Emulsion Stability. *J Colloid Interf Sci* **285** (2): 821–833. http://goo.gl/LLEPLa.

Thawer, R., Nicoll, D. C. and Dick, G. 1990. Asphaltene Deposition in Production Facilities. *SPE Production Engineering* **5** (4): 475–480. SPE-18473-PA. http://dx.doi.org/10.2118/18473-PA.

Vannaxay, D., Wasden, F. K. and Howell, B. 2014. Carmon Creek Thermal Field Development Project. Presented at the SPE Annual Technical Conference and Exhibition, 27-29 October, Amsterdam, The Netherlands. SPE-170879-MS. http://dx.doi.org/10.2118/170879-MS.

Wang, C. and Leung, J. 2015. Characterizing the Effects of Lean Zones and Shale Distribution in Steam-Assisted-Gravity-Drainage Recovery Performance. *SPE Reserv Eval Eng* **18** (3): 329–345. SPE-170101-PA. http://goo.gl/mYJHnz.

Wiebe, R. and Gaddy, V. L. 1940. The Solubility of Carbon Dioxide in Water at Various Temperatures from 12 to 40 and at Pressures to 500 Atmospheres. Critical Phenomena. *J Am Chem Soc* **62** (4): 815–817. http://goo.gl/nTJEyB.

Wightman, D., Rottenfusser, J., Kramers, J. and Harrison, R. 1989. In *AOSTRA Technical Handbook on Oil Sands, Bitumens and Heavy Oils*. ed. L. G. Hepler and C. Hsi. Edmonton, Alberta, Canada: Alberta Oil Sands Technology and Research Authority.

Yang, C. and Gu, Y. 2006. Diffusion Coefficients and Oil Swelling Factors of Carbon Dioxide, Methane, Ethane, Propane and their Mixtures in Heavy Oil. *Fluid Phase Equilibr* **243** (1): 64–73. http://dx.doi.org/10.1016/j.fluid.2006.02.020.

Yong, W. P. and Awang, M. 2014. Water/Carbon Dioxide Phase Equilibria using Thermodynamic Perturbation Theory. *Journal of Applied Sciences* **14** (22): 3055-–3062. http://dx.doi.org/10.3923/jas.2014.3055.3062.

APPENDIX A

CONTROL TGA/DSC RESULTS FOR DISTILLED WATER

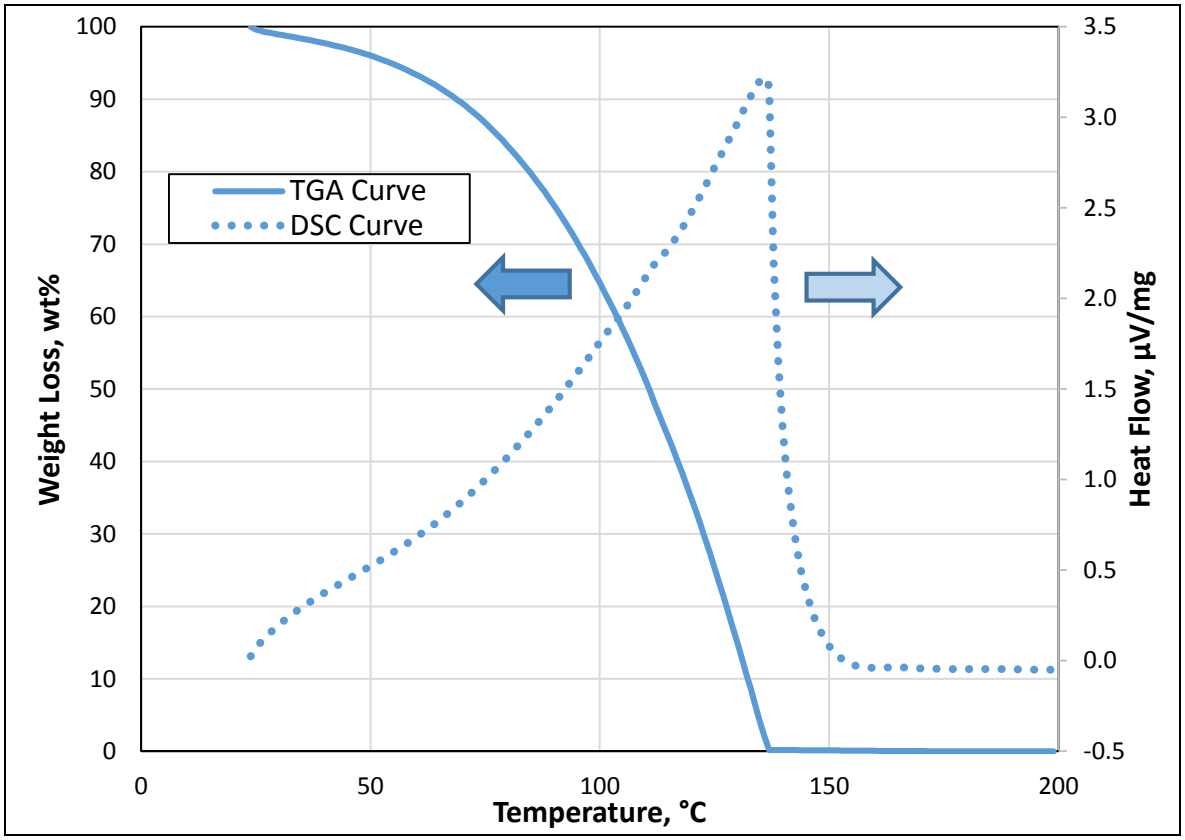

Figure A-1. TGA/DSC analysis of distilled water.

APPENDIX B

RHEOLOGICAL BEHAVIOR OF PRODUCED OIL

B1. Rheological Behavior.

Table B-1. Regressed flow consistency and flow behavior indexes for produced oil samples.

Oil Sample	K	n	R^2
Original Oil	4.198	0.977	1.000
E1: Steam-flooding	19.579	0.717	0.993
E2: Propane Flooding	4.030	0.961	0.999
E3: CO_2 Flooding	87.277	0.326	0.951
E4: 1:9 Propane-Steam	715.990	0.833	0.996
E5: 1:1 Propane-Steam	23.049	0.861	0.999
E6: 9:1 Propane-Steam	46.674	0.849	1.000
E7: 9:1 CO_2-Steam	25.266	0.998	1.000
E8: Steam-flooding - No Clays	55.874	0.839	1.000
E9: Propane Flooding - No Clays	8.808	0.881	1.000
E10: CO_2 Flooding - No Clays	10.534	0.871	0.999
E11: 9:1 Propane-Steam - No Clays	58.673	0.997	1.000
E12: 9:1 CO_2-Steam - No Clays	39.137	0.943	0.999

B2. Measured *versus* calculated viscosity of produced oil samples.

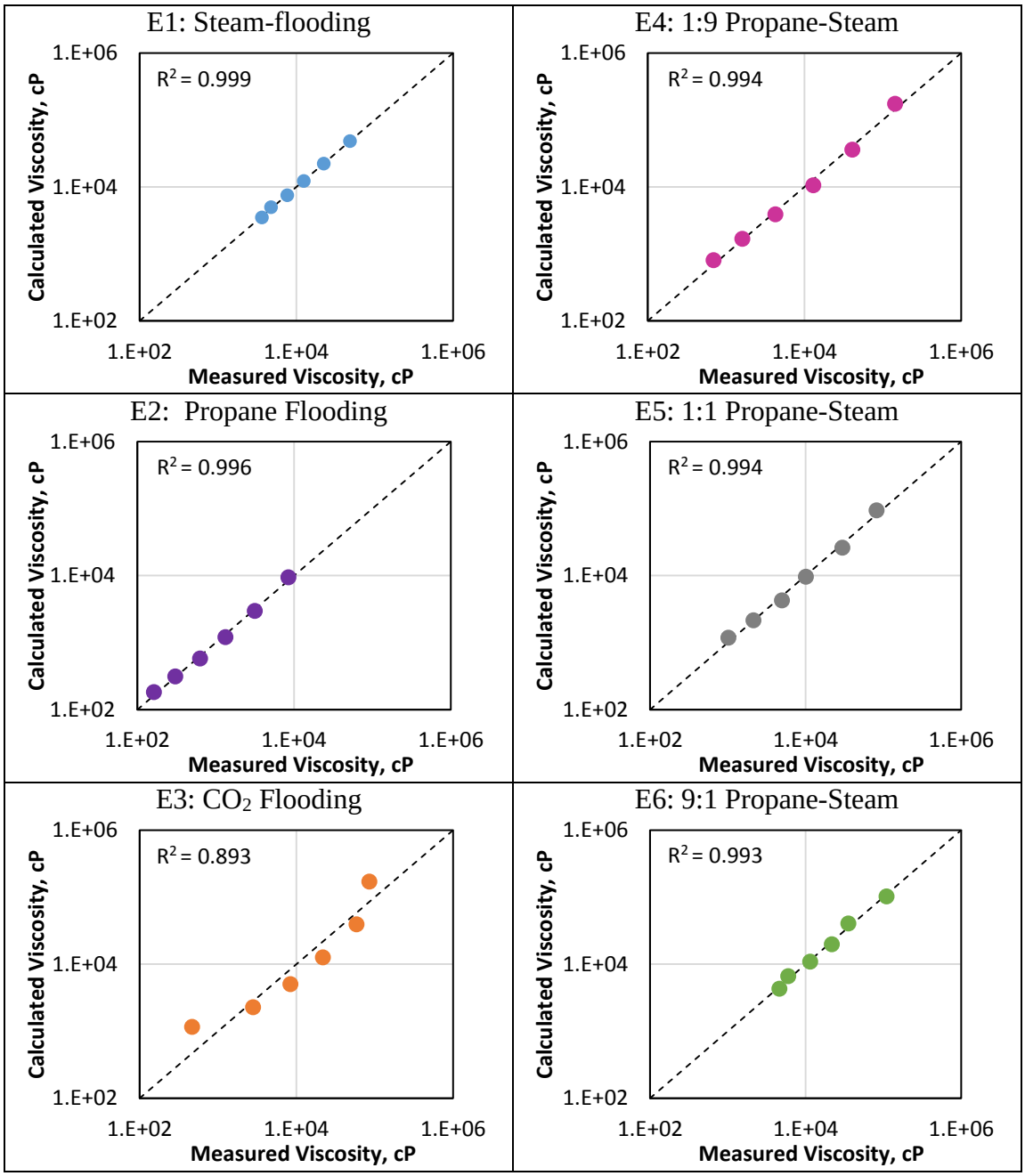

Figure B-1. Comparison of calculated and measured viscosities of produced oil samples (experiments E1, E2, E3, E4, E5, and E6). Dashed lines represent perfect fit.

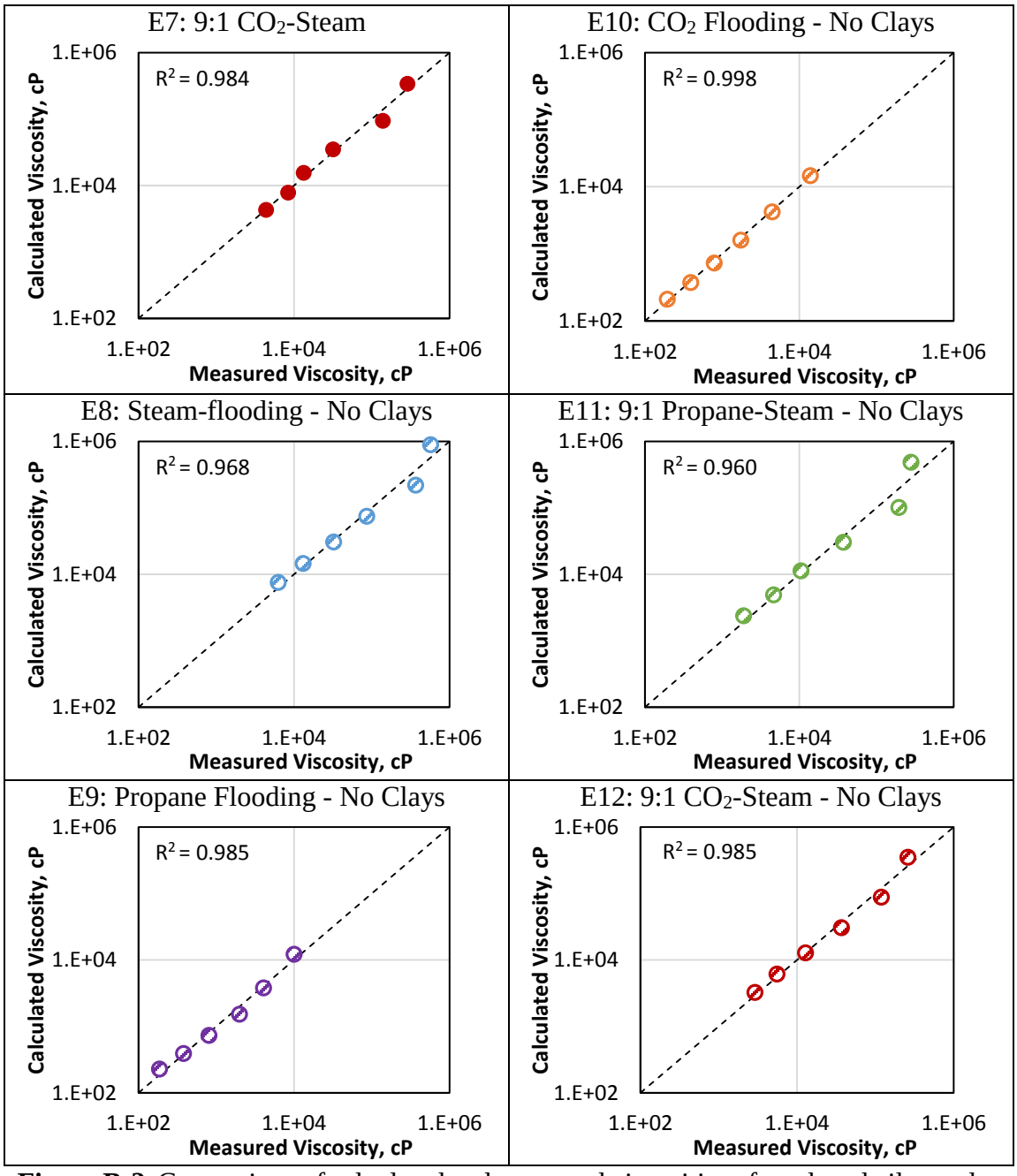

Figure B-2. Comparison of calculated and measured viscosities of produced oil samples (experiments E7, E8, E9, E10, E11, and E12). Dashed lines represent perfect fit.

APPENDIX C

TGA/DSC RESULTS

This appendix presents the TGA/DSC results for the produced oil, precipitated asphaltenes, and spent-rock samples.

While the samples are heated at a constant heating rate of 5 °C/min, the TGA and DSC results are reported. While the TGA curve represents the weight loss, the DSC curve represents the heat flow during sample combustion.

In the DSC curve, peaks are indicative of endothermic reactions, with energy being adsorbed by the sample to break chemical bonds or to cause phase transitions. Valleys indicate exothermic reactions, in which thermal energy is released from the chemical bonds (Kar and Hascakir, 2015; Klock and Hascakir, 2015).

C1. TGA/DSC Analysis for Produced Oil Samples

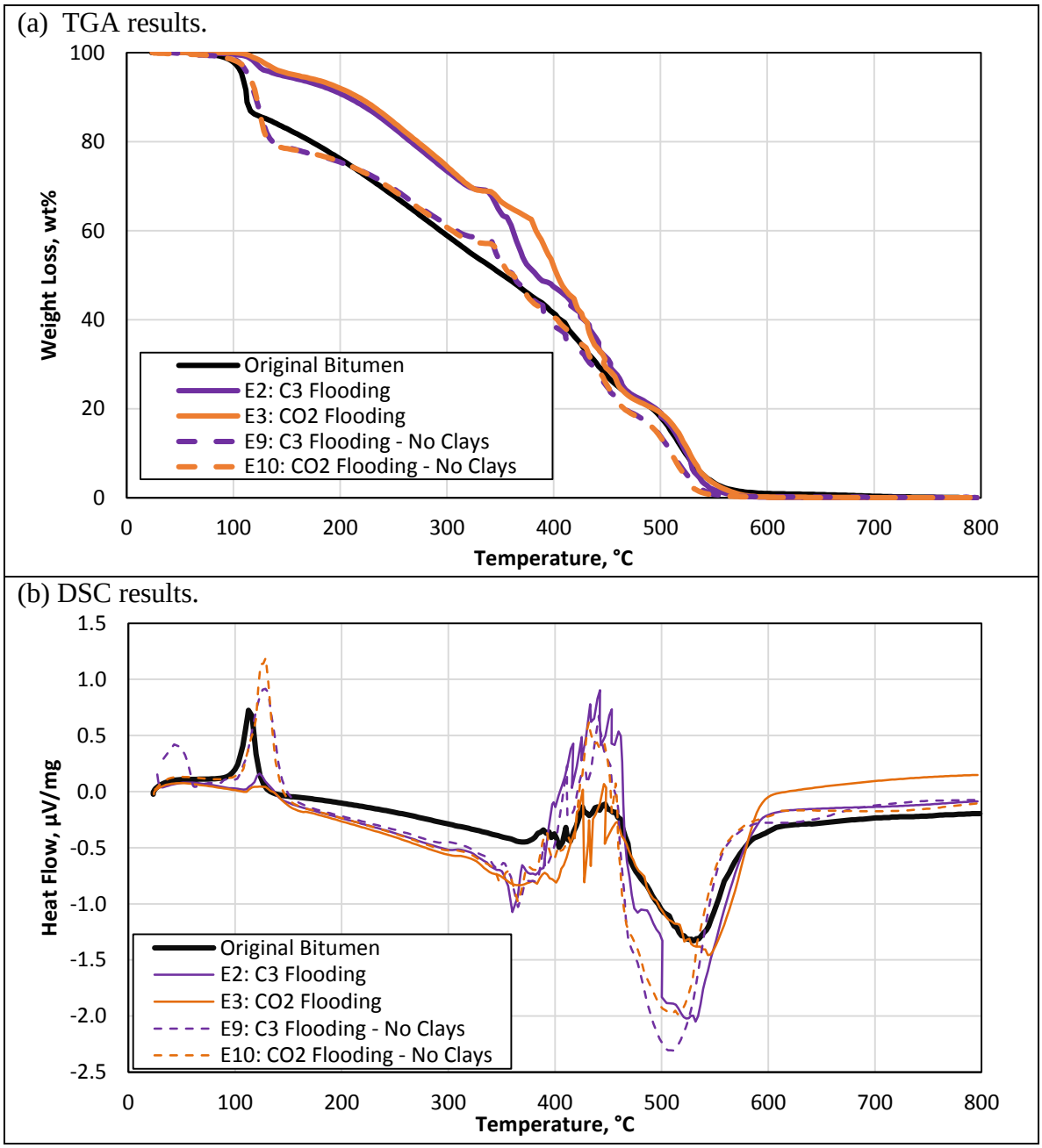

Figure C-1. TGA/DSC analysis of produced oil samples from solvent flooding experiments (E2, E3, E9, and E10).

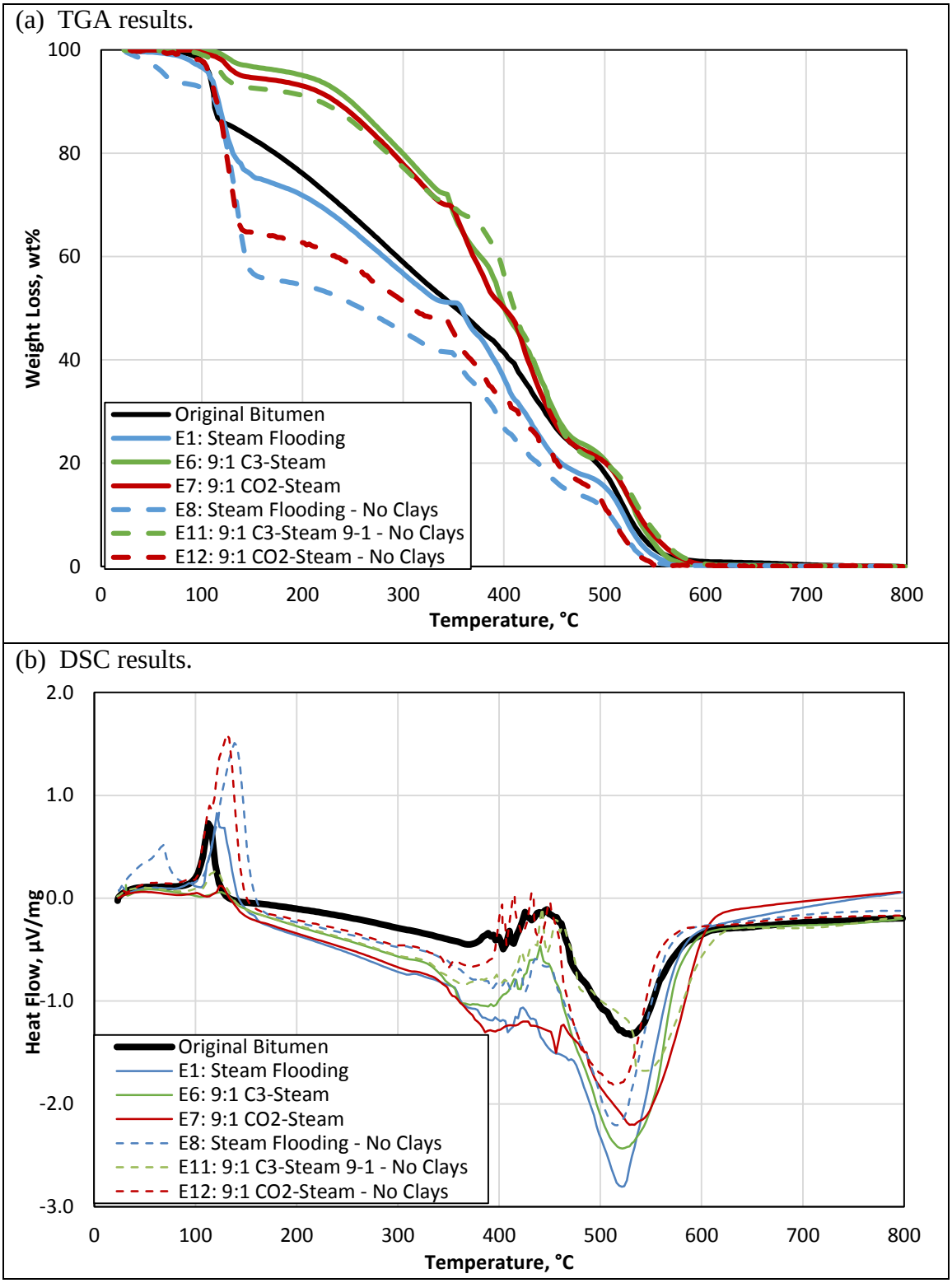

Figure C-2. TGA/DSC analysis of produced oil samples from steam and solvent-steam-flooding experiments (E1, E6, E7, E8, E11, and E12).

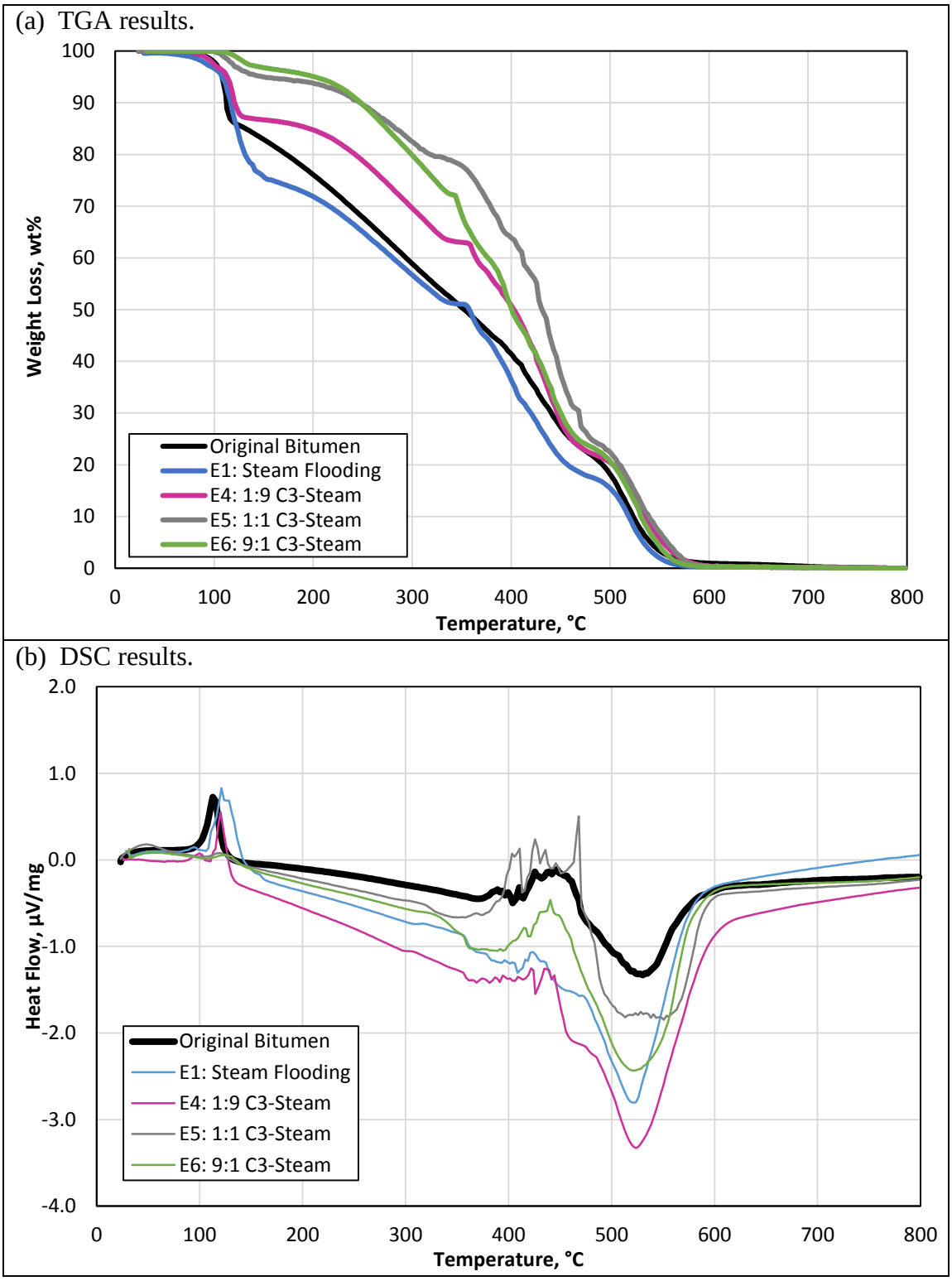

Figure C-3. TGA/DSC analysis of produced oil samples from steam and propane-steam-flooding experiments (E1, E4, E5, and E6).

C2. TGA/DSC Analysis for Asphaltenes Precipitated under Solvent Flooding

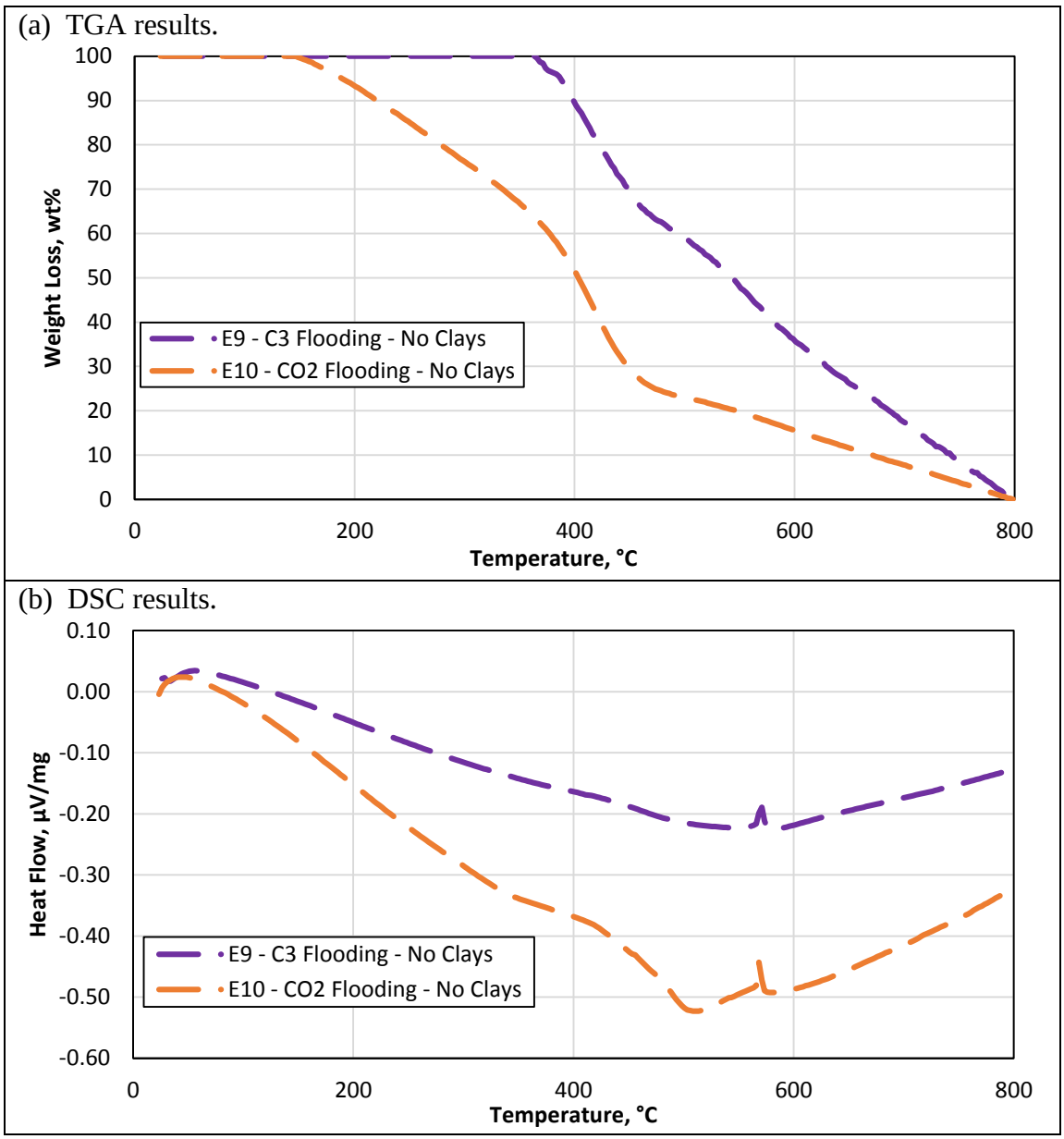

Figure C-4. TGA/DSC analysis of precipitated asphaltenes from solvent flooding experiments without clays.

C3. TGA/DSC Analysis for Postmortem Samples

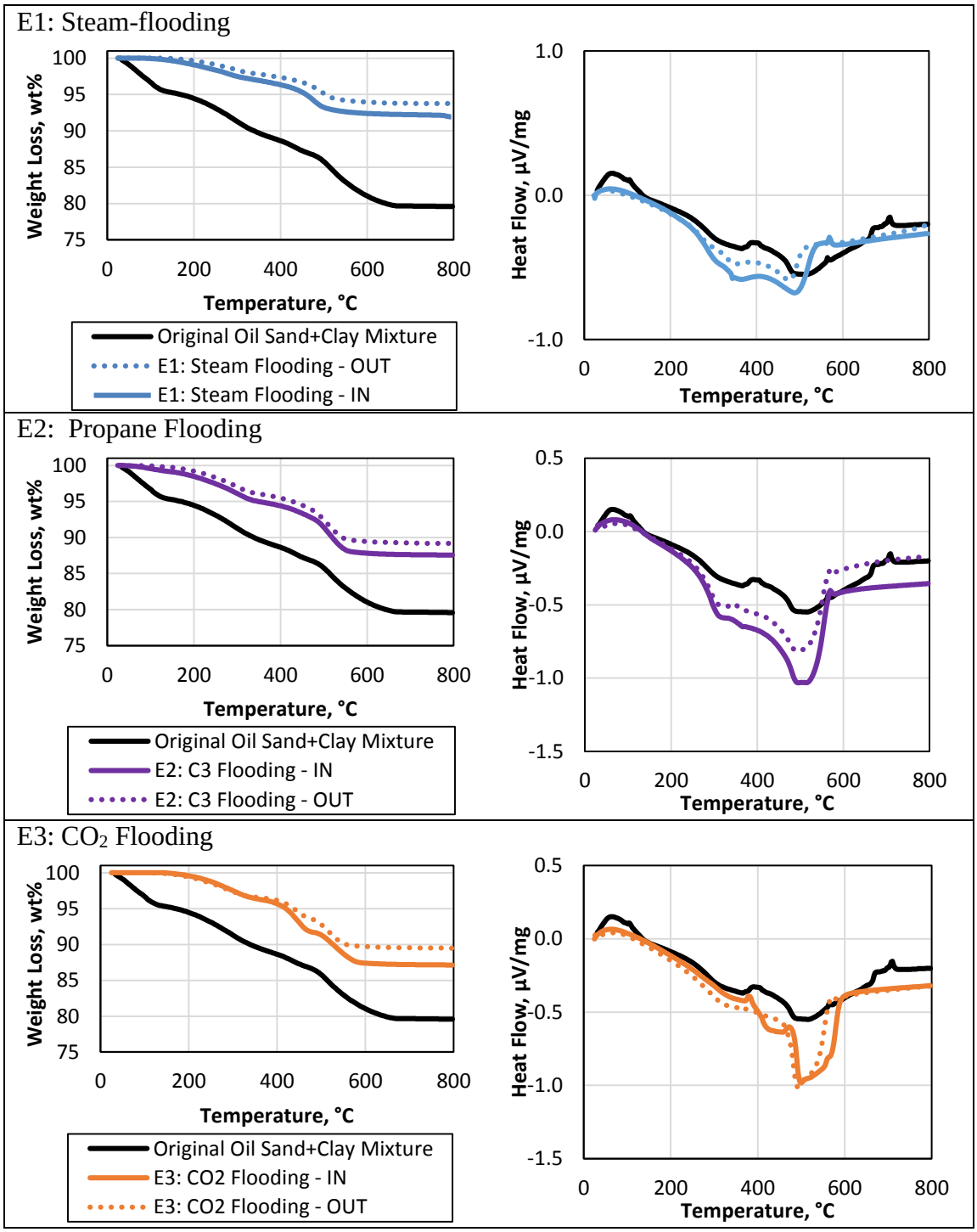

Figure C-5. TGA/DSC analysis of postmortem samples from experiments E1, E2, and E3.

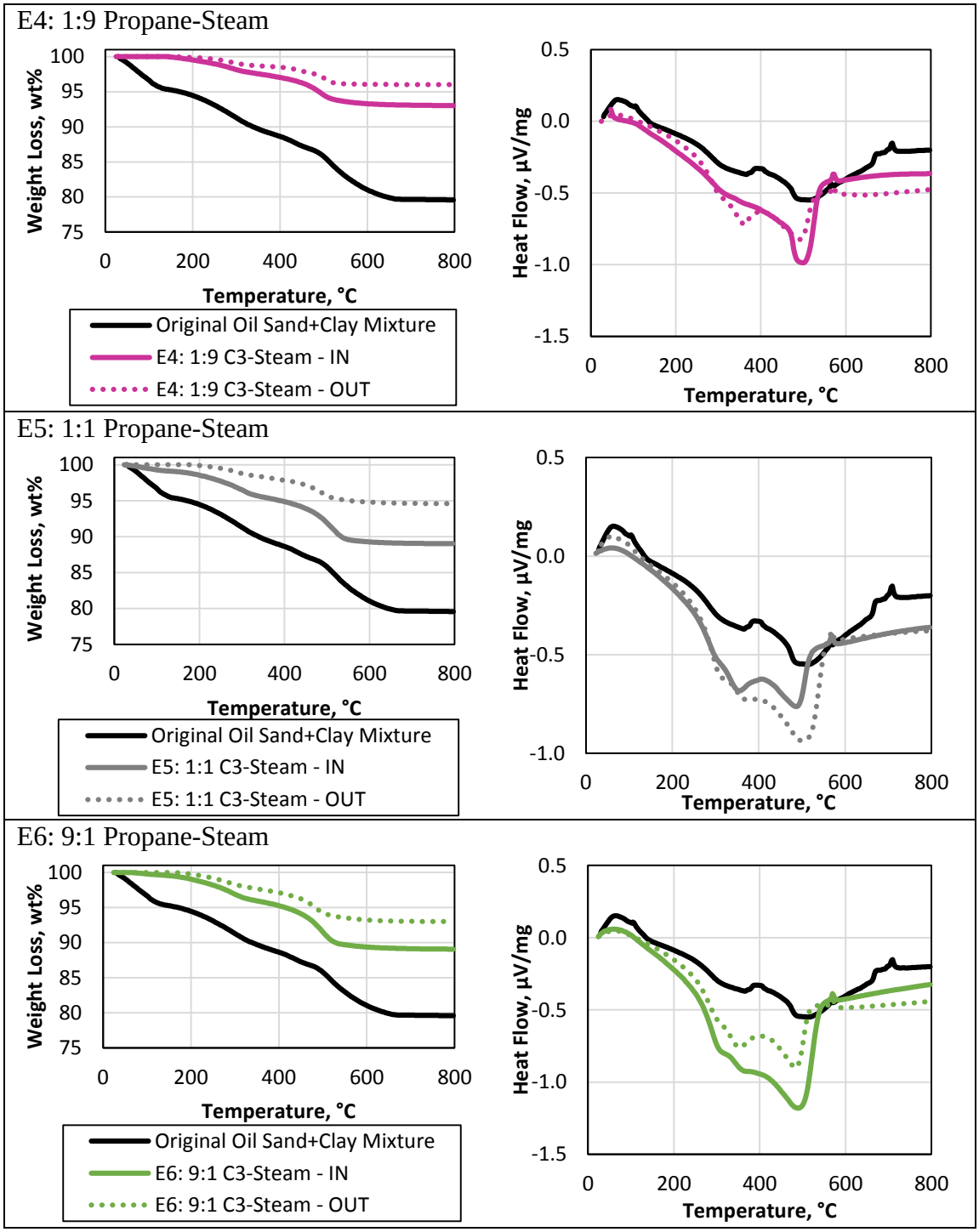

Figure C-6. TGA/DSC analysis of postmortem samples from experiments E4, E5, and E6.

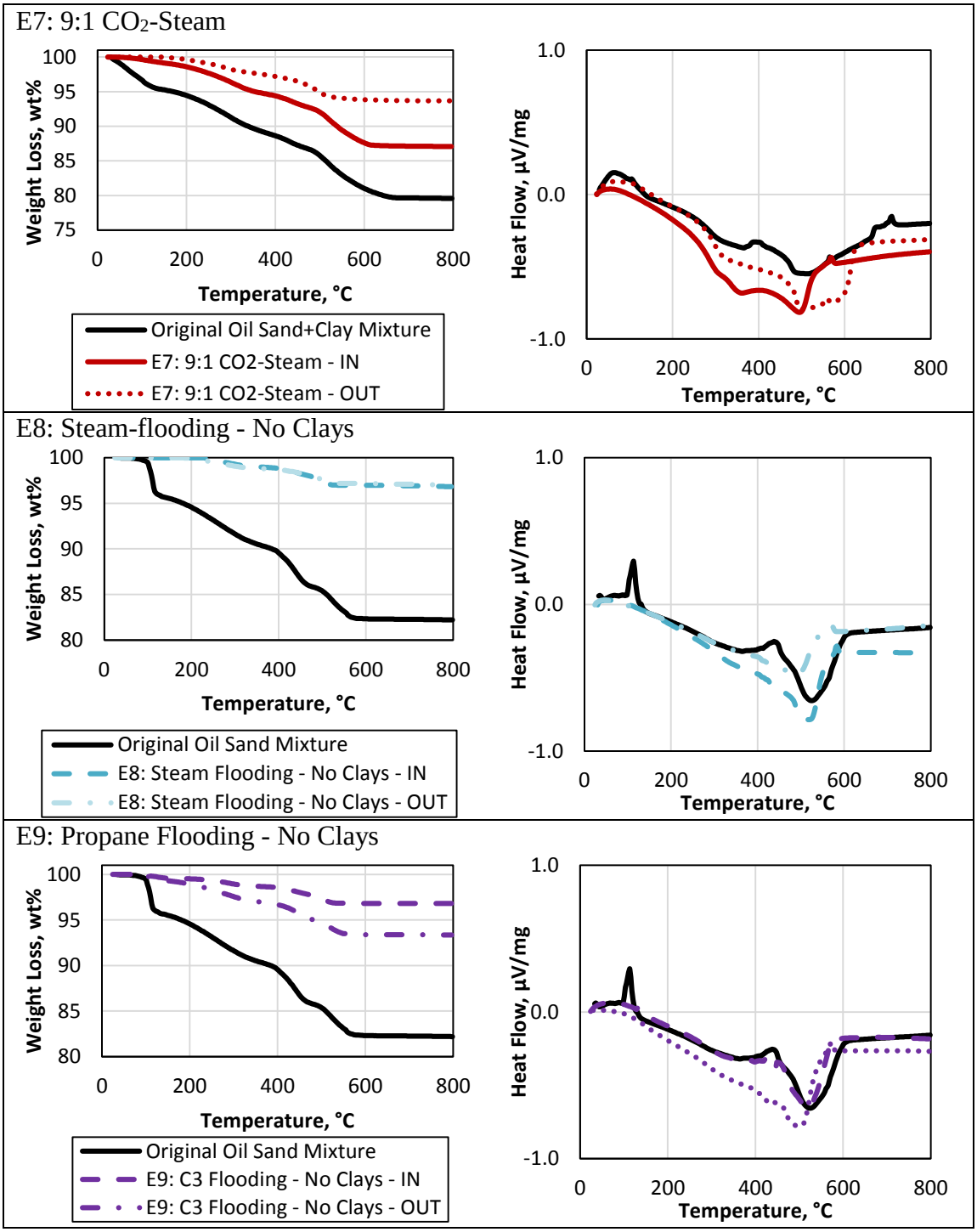

Figure C-7. TGA/DSC analysis of postmortem samples from experiments E7, E8, and E9.

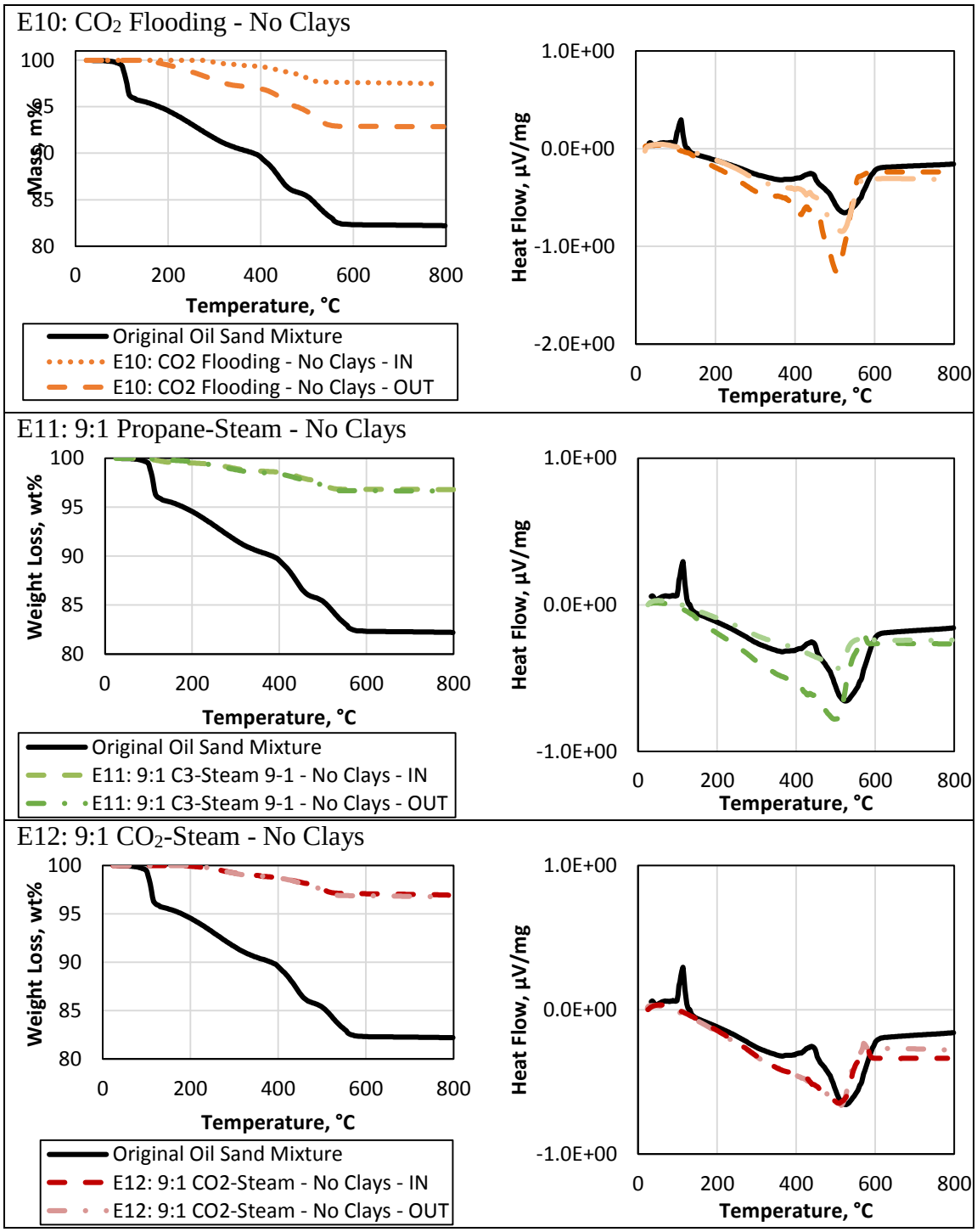

Figure C-8. TGA/DSC analysis of postmortem samples from experiments E10, E11, and E12.

APPENDIX D

PHASE BEHAVIOR CALCULATIONS

A single pseudo-component was chosen to represent the actual Peace River dead oil bitumen sample used in the experiments (Table D-1).

Using PVTSim Nova software, several Vapor-Liquid Equilibrium (VLE) flash calculations were performed for the CO_2/propane/Peace River bitumen mixture by maintaining temperature and pressure fixed and varying molar compositions.

To reproduce the experimental conditions (Table 2), the first calculations were made at 20°C and 14.7 psi (solvent injection experiments), as well as at 115°C and 14.7 psi (steam and solvent-steam experiments). To mimic the Peace River reservoir conditions, a second set of calculations were made at 17°C and 550 psi (Hamm and Ong, 1995) to represent pure solvent injection. To simulate steam injection conditions in the field conditions, a final set of flash calculations were ran at 262°C and 550 psi.

Table D-1. Peace River pseudo-component fluid properties (Li et al., 2013).

Property, unit	**Value**
Molecular weight	542
Specific gravity @15.6°C	0.9974
Critical temperature, °C	678.94
Critical pressure, psi	161.76
Acentric factor	1.1016

The VLE flash calculations were performed using Peng Robinson Equation-of-State (PR-EOS) with Peneloux volume translation (Peneloux et al., 1982).

Despite the high asphaltene content of Peace River bitumen, the formation of asphaltene-rich phases and the solvent-water solubility were not considered in these simulations.

For a more comprehensive phase behavior simulation, the asphaltene precipitation may be modelled as a pure solid or dense liquid phase (Nghiem and Coombe, 1997; Pedersen et al., 2006), whereas solvent-water solubility could be accurately modelled by using Cubic-Plus-Association Equation-of-State (Kontogeorgis et al., 1996; Yong and Awang, 2014; Hajiw et al., 2015).

The results of the multiphase, multicomponent flash are used to build the pseudo-ternary diagrams by inputting the molar composition of each phase (liquid or vapor) at the calculated equilibrium states.

Though actual CO_2/propane/Peace River bitumen are not tested experimentally in this study, the representation with pseudo-ternary diagrams was chosen for its simplicity.

The maximum molar concentration of either solvents in the oil-rich liquid phase is the final estimated solvent solubility. Results are presented in Table D-2 and visually represented in Figure D-1 as pseudo-ternary diagrams.

Results in Table D-2 demonstrate that for all simulated conditions, propane is more soluble in Peace River than CO_2, indicating the higher chemical affinity of bitumen to the hydrocarbon than to the non-hydrocarbon solvent.

Despite the higher propane solubility with oil than CO_2 at the simulated experimental conditions, immiscible conditions prevail both for both solvents. For the pure solvent injection, only 12.96 mole% of pure propane or 1.51 mole% of pure CO_2 would be soluble with Peace River dead oil (Figure D-1a). For the steam and solvent-steam experiments, the solubilities for pure propane and pure CO_2 with Peace River bitumen are estimated at 2.56 and 0.59 mole%, respectively (Figure D-1b).

Table D-2. Estimated solubilities for propane and CO_2 in Peace River dead oil.

Condition	**Temperature, °C**	**Pressure, psi**	**Propane solubility in Peace River, mole%**	**CO_2 solubility in Peace River, mole%**
Experimental (Solvent injection)	20	14.7	12.96	1.51
Experimental (Steam and solvent-steam-flooding)	115	14.7	2.56	0.59
Reservoir (Solvent injection) (Hamm and Ong, 1995)	17	550	100	46.51
Reservoir (Steam and solvent-steam-flooding) (Hamm and Ong, 1995)	262	550	28.12	12.19

Complete solvent-bitumen miscibility is only achieved for the reservoir conditions simulating pure propane injection (Figure D-1c). For this same condition, only 46.51 mole% of CO_2 would be soluble in oil.

Such results indicate that for the experimental studies conducted in this work, the usage of either solvent did not achieve oil miscible displacement, which is more favorable than the immiscible type displacement (Green and Willhite, 1998).

It must also be mentioned that for the actual field scale applications, the Peace River reservoir bitumen contains dissolved gases (Svrcek and Mehrotra, 1989; Vannaxay et al., 2014). Therefore, the solubilities of propane and CO_2 solvents with live oil are expected to be higher than those presented in Table D-2. However, the solubility results for dead oil can still be used as first estimates to qualitatively understand the solvent-bitumen phase behavior.

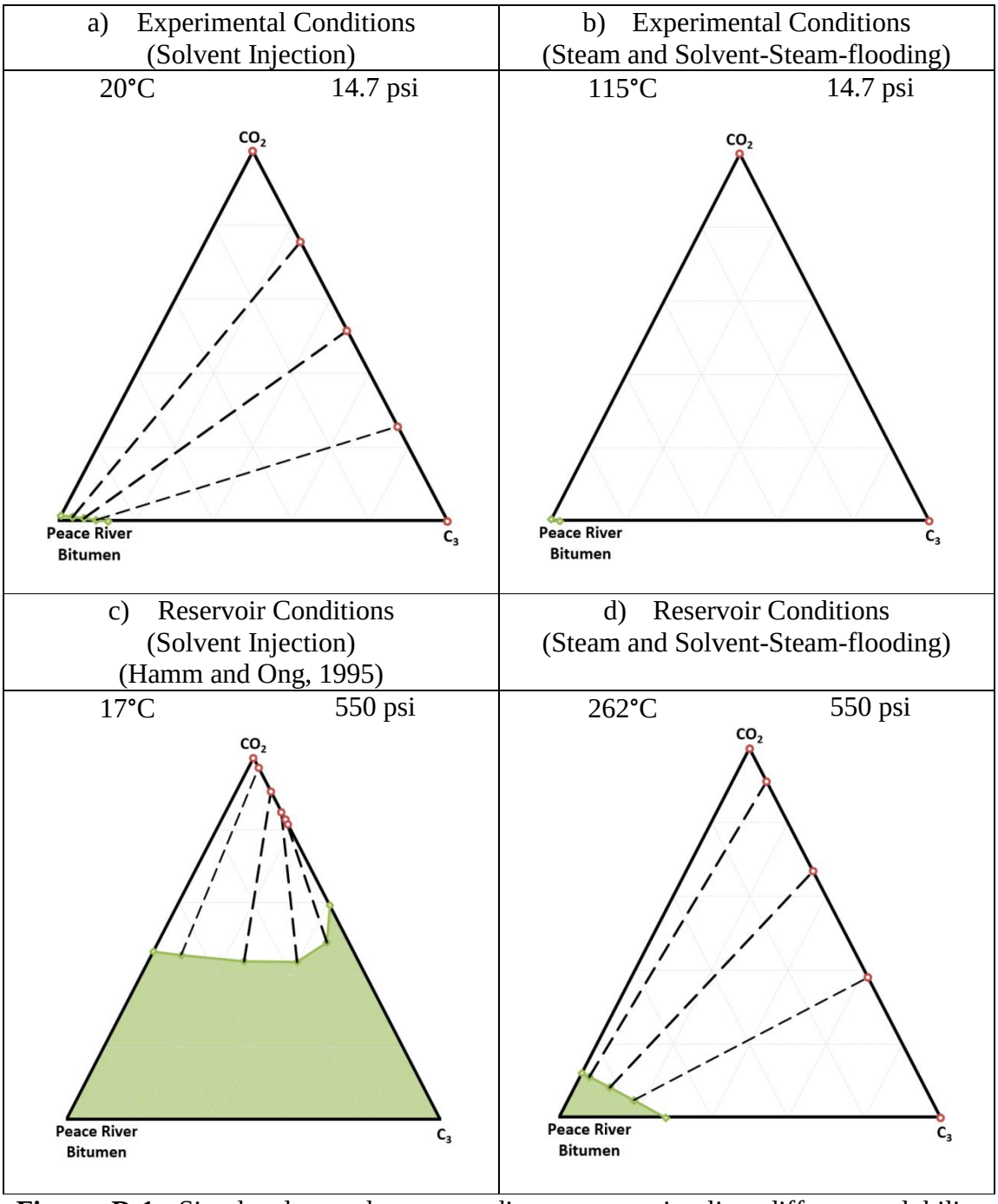

Figure D-1. Simulated pseudo-ternary diagrams to visualize different solubility behaviors of propane and CO_2 with Peace River bitumen.

APPENDIX E

REPEATABILITY

To investigate the repeatability of the results, experiments E1 (steam-flooding, sand-clay rock) and E5 (1:1 propane-steam, sand-clay rock) were repeated. The recovery performance results are presented in Figure E-1.

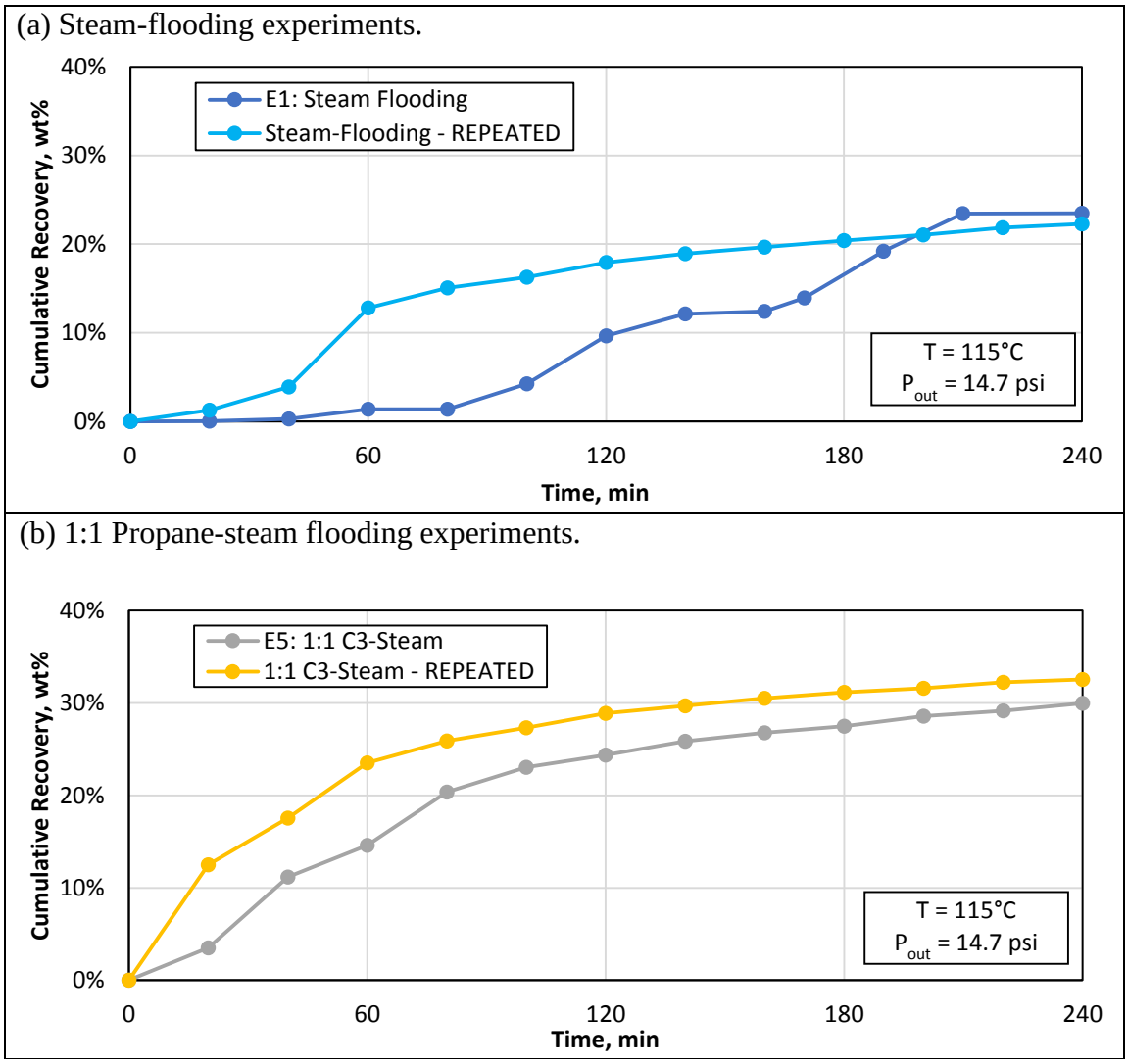

Figure E-1. Cumulative oil recovery (clays and water excluded) for repeated experiments.

For the steam-flooding experiments, Figure E-1 demonstrates that the recovery performance curves are different for the original and the repeated experiments. However, despite the original experiment displayed longer delay on oil production, the ultimate oil recovery for both cases are similar: 23.5 wt% for the original case and 22.3 wt% for the repeated one.

Similar observations are made for the 1:1 Propane-Steam experiments, as the repeated case had 33.0 wt% ultimate oil recovery, while the original experiment achieved 30 wt%.

Such differences may be explained by heterogeneities in the reservoir rock, as the sand-clay mixtures are manually prepared and packed.

However, the repeatability results also indicate that, despite the variations, the main conclusions from this work remain valid. Both the steam-flooding cases experienced delayed and reduced recovery as compared to SSF cases and to steam-flooding without clays. Additionally, both 1:1 propane-steam cases had worse performance than 1:9 propane-steam (E4), but slightly higher recovery than the 9:1 propane-steam experiment (E6).